



HAL
open science

Trends and progress in AnMBR for domestic wastewater treatment and their impacts on process efficiency and membrane fouling

Fatima Anjum, Irfan Khan, Jeonghwan Kim, Muhammad Aslam, Gaetan Blandin, Marc Heran, Geoffroy Lesage

► To cite this version:

Fatima Anjum, Irfan Khan, Jeonghwan Kim, Muhammad Aslam, Gaetan Blandin, et al.. Trends and progress in AnMBR for domestic wastewater treatment and their impacts on process efficiency and membrane fouling. *Environmental Technology and Innovation*, 2021, 21, pp.101204. 10.1016/j.eti.2020.101204 . hal-04065120

HAL Id: hal-04065120

<https://hal.umontpellier.fr/hal-04065120>

Submitted on 9 Oct 2023

HAL is a multi-disciplinary open access archive for the deposit and dissemination of scientific research documents, whether they are published or not. The documents may come from teaching and research institutions in France or abroad, or from public or private research centers.

L'archive ouverte pluridisciplinaire **HAL**, est destinée au dépôt et à la diffusion de documents scientifiques de niveau recherche, publiés ou non, émanant des établissements d'enseignement et de recherche français ou étrangers, des laboratoires publics ou privés.

Trends and progress in AnMBR for domestic wastewater treatment and their impacts on process efficiency and membrane fouling

Fatima Anjum¹, Irfan M. Khan¹, Jeonghwan Kim², Muhammad Aslam³, Gaetan Blandin^{1,4}, Marc Heran¹, Geoffroy Lesage¹.

¹IEM, Univ Montpellier, CNRS, ENSCM, Montpellier, France

²Department of Environmental Engineering, Inha University, Incheon, Republic of Korea

³Department of Chemical Engineering, COMSATS University Islamabad (CUI), Lahore Campus, Defense Road, Off Raiwind Road, Lahore, Pakistan

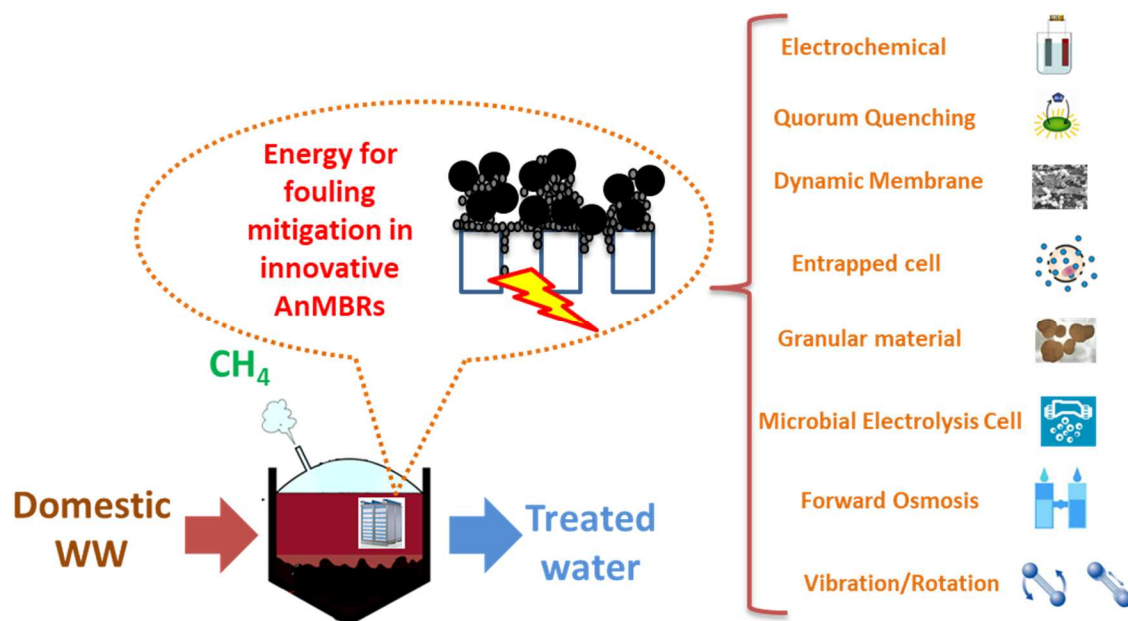
⁴Eurecat, Centre Tecnològic de Catalunya, Water, Air and Soil Unit, Manresa, Spain

*corresponding author: geoffroy.lesage@umontpellier.fr

Keywords

Anaerobic Membrane Bioreactor, Domestic wastewater treatment, Fouling, Hybrid processes, Biogas.

Graphical abstract



Abstract

Anaerobic membrane bioreactor has emerged as an innovative technology in treating domestic wastewater due to its excellent produced effluent quality and high potential of neutral or positive energy balance. One of the biggest challenges in positive energy objective is fouling mitigation which contributes towards 70% of the total energy requirement of MBR-

22 based domestic wastewater treatment. Numerous studies were carried out to address this
 23 issue, utilizing various reactor design configurations and operating conditions for energy
 24 minimization as well as membrane performance enhancement. The latest research trend in
 25 this sector is the establishment of hybrid processes like Granular Anaerobic Membrane
 26 Bioreactors (G-AnMBR), Forward Osmosis Anaerobic Membrane Bioreactor (FO-AnMBR)
 27 and Microbial Electrolysis Cell - Anaerobic Membrane Bioreactor (MEC-AnMBR) for
 28 domestic wastewater treatment which not only provides efficiency in treatment but also
 29 improves fouling mitigation. Also, the application of techniques developed particularly for
 30 fouling mitigation like quorum quenching and sensing, cell entrapment and membrane
 31 module vibrations in AnMBRs were assessed. This paper reviews the latest trends in
 32 anaerobic membrane bioreactors research with regards to water quality produced, removal
 33 efficiencies and fouling mitigation.

34 **Table of Contents**

35 1. Introduction.....5
 36 2. Current status of operation and fouling in pilot-scale AnMBR.....9
 37 2.1. Configuration models of pilot-scale AnMBRs for fouling control.....9
 38 2.2. Fouling mechanisms in pilot-scale AnMBRs.....10
 39 2.3. Fouling mitigation strategies in pilot-scale AnMBRs.....12
 40 2.3.1. Scouring methods.....12
 41 2.3.2. Filtration cycles in AnMBRs13
 42 2.3.3. Chemical cleaning cycles.....13
 43 2.4. Removal of organics in pilot-scale AnMBRs14
 44 2.5. Energy requirements in the pilot-scale AnMBRs for fouling mitigation.....15
 45 3. Novel AnMBRs for fouling mitigation.....16
 46 3.1. Granular-AnMBR.....18
 47 3.1.1. G-AnMBR v/s Conventional AnMBR.....19
 48 3.1.2. Effect of configuration on fouling in G-AnMBR20
 49 3.1.3. Effect of gas sparging regime on performance and energy demand in G-
 50 AnMBR
 51 3.1.4. Sponge assisted G-AnMBR22
 52 3.2. Entrapped cell AnMBR.....24

53	3.3. Dynamic AnMBR	25
54	3.3.1. DM layer formation mechanism in AnDMBR	25
55	3.3.2. Submerged versus external dynamic AnMBR.....	26
56	3.3.3. Effect of operating conditions in AnDMBR.....	27
57	3.3.4. Fouling mechanism in AnDMBR	29
58	3.3.5. Fouling mitigation in AnDMBR.....	30
59	3.4. Forward Osmosis AnMBR (FO-AnMBR).....	31
60	3.4.1. Configuration and working principle of FO-AnMBR	31
61	3.4.2. Performance comparison of FO-AnMBR with conventional AnMBR	34
62	3.4.3. Fouling and salinity build-up in FO-AnMBR.....	35
63	3.4.4. Fouling mitigation in FO-AnMBR	36
64	3.4.5. Salinity build-up mitigation in FO-AnMBR.....	37
65	3.5. Microbial Electrolysis Cell-AnMBR	38
66	3.6. Anaerobic Electrochemical Membrane Bioreactor (AnEMBR).....	41
67	3.7. Vibration application in AnMBR.....	44
68	3.8. Biological mitigation – Quorum Quenching.....	47
69	4. Future perspective.....	50
70	5. Conclusion	51
71	Acknowledgments.....	52
72	References.....	59

73

74

75 **Table of Abbreviations**

76	AeMBR: Aerobic membrane bioreactor
77	AHL: N-acryl homoserine lactone
78	AnDMBR: Anaerobic dynamic membrane bioreactor
79	AnEMR: Anaerobic electrochemical membrane bioreactor
80	AFMBR: Anaerobic fluidized membrane bioreactor
81	AnGS: Anaerobic granular sludge
82	AnMBR: Anaerobic membrane bioreactor
83	ATP: Adenosine triphosphate
84	BB: Building blocks
85	GSP: Biogas sparging
86	CFV: Crossflow velocity
87	COD: Chemical oxygen demand
88	CSTR: Continuous stirred tank reactor
89	DLVO: Derjaguin, Landau, Verwey, and Overbeek
90	DM: Dynamic membrane
91	DWW: Domestic wastewater
92	DWWT: Domestic wastewater treatment

93 EB: Empty beads
94 EG-AnMBR: Externally submerged granular AnMBR
95 IG-AnMBR: Internally submerged granular AnMBR
96 ES-AnMBR: Externally submerged membrane bioreactor
97 EPS: Extracellular polymeric substances
98 F/M ratio: Food to microorganism ratio
99 FO-AnMBR: Forward Osmosis Anaerobic Membrane Bioreactor
100 GAC: Granular activated carbon
101 G-AnMBR: Granular anaerobic membrane bioreactor
102 GHG: Greenhouse gases
103 GSI_m: Biogas sparging intensity
104 GSP: Biogas sparging
105 HRT: Hydraulic residence time
106 LMH: Liter per square meter per hour
107 LMW: Low molecular weight
108 MF: Microfiltration
109 MEC: Microbial electrolysis cell
110 MEC-AnMBR: Microbial Electrolysis Cell - Anaerobic Membrane Bioreactor
111 MLSS: Mixed liquor suspended solids
112 MMV: Magnetically induced membrane vibration
113 MT: Membrane tank
114 MWh: Megawatt hour
115 P/C ratio: Protein to carbohydrate ratio
116 PSP: Particle sparging
117 PVDF: Polyvinylidene difluoride
118 QQ: Quorum quenching
119 QQB: Quorum quenching beads
120 RMEM: Rotating membrane
121 SCSA: Specific cathode surface area
122 SDG: Sustainable development goal
123 SG-AnMBR: Internally submerged granular AnMBR
124 SMP: Soluble microbial products
125 SRT: Solid retention time
126 TMP: Trans-membrane pressure
127 UASB: Up-flow anaerobic sludge blanket
128 UF: Ultrafiltration
129 VLR: Volumetric Loading Rate
130 VSEP: Vibratory shear enhancement process
131 WWTP: Wastewater Treatment Plants
132 WRRF: Water Resource Recovery Facilities
133

134 **1. Introduction**

135 In 2015, United Nations adopted the 2030 Agenda for Sustainable Development (SD) (UN
136 2019); SD Goal (SDG) 6 aims at ensuring availability and sustainable management of water
137 and sanitation for all. To help address these issues, domestic wastewater (DWW) is thus now
138 considered to be an alternative water (SDG 6), nutrients (SDG 2) and energy (SDG 7) source
139 for various applications. Wastewater Treatment Plants (WWTPs) have even been rebranded
140 as Water Resource Recovery Facilities (WRRFs) to enlighten the significant resource
141 recovery potential that exists in DWW streams (Jain, 2018; Fulcher, 2014). The biological
142 treatments such as aerobic and partial nitrification-anammox granular sludge are becoming
143 increasingly popular in DWW treatment due to their high tolerance of the toxicity of feed,
144 compactness, settling efficiencies and effectiveness in treating complex effluents with high
145 organic load and low biodegradable compounds (Baeten et al., 2019; Taghipour, 2017;
146 Taghipour and Ayati, 2017; Zhang et al., 2016). However, aerobic processes are highly
147 energy-intensive and produce a large amount of sludge (Kim et al., 2011).

148 Recently, a change of paradigm was made from reliance on aerobic treatment towards
149 anaerobic treatment which uses organic carbon from the DWW to produce energy in the form
150 of methane gas and reduces the amount of sludge to be handled. However, anaerobic
151 treatment alone may not be enough to meet stringent discharge limits and to hold anaerobic
152 micro-organisms that have a very slow-growth rate. The introduction of membrane
153 technology into anaerobic bioreactor is a promising solution to these issues.

154 Since more than twenty years, Anaerobic Membrane Bioreactors (AnMBRs) are in operation
155 for the treatment of high strength WW i.e. industrial and agricultural WW (Amha et al., 2019;
156 Bu et al., 2017; Thongmak et al., 2016). Kanai et al., (2010) have presented the successful
157 demonstration of Kubota's submerged anaerobic membrane biological reactor (a patented
158 technology with 15 full-scale plants) at a spillage treatment plant in Japan. In addition to that

159 its' applications include food waste and garbage treatment. The technology combines
160 submerged membrane separation and anaerobic digestion in a single unit with a COD
161 removal efficiency of up to 92% and an energy recovery of around 12 GJ/d. Christian et al.,
162 (2011) have reported the two years operation of a full-scale AnMBR treating food industry
163 wastewater achieving 99% COD removal and resulting in up to 50% reduction in the total
164 operating expenses of the wastewater treatment plant facility. For domestic wastewater
165 treatment, no full-scale plant has been commissioned so far owing to the highly variable feed
166 conditions and fouling issues. Robles et al., (2018) have underlined the need of further works
167 on fouling behavior understanding, fouling mitigation and process control in AnMBRs for
168 DWW treatment. New trends in circular economy calls for the utilization of AnMBR for
169 domestic wastewater treatment since AnMBRs are able to:

- 170 • Retain anaerobic bacteria completely (Hydraulic and Solid Retention Time (HRT and
171 SRT) are uncoupled in AnMBR) and work with higher loading capacity;
- 172 • Produce excellent permeate qualities (i.e. high removal of suspended solids, organic
173 matter and microorganisms) thanks to microfiltration (MF) or ultrafiltration (UF)
174 membranes (Lim et al., 2020);
- 175 • Keep the nutrients of the influent available for their recovery or direct reuse (e.g. struvite
176 crystallization, microalgae cultivation, fertigation...) (Judd et al., 2015);
- 177 • Reduce Green House Gas (GHG) emissions by saving energy consumption: net energy
178 production of 0.1 kWh/m³ with AnMBR when aerobic treatment consumes approximately
179 0.25-0.6 kWh/m³ of treated DWW (Pretel et al., 2016; McCarty et al., 2011).
- 180 • Reduce the amount of sludge to dispose of due to the lower growth yield of the anaerobic
181 biomass (up to 90% reported by a study (Jeison et al., 2008));
- 182 • Reduce footprint due to higher compacity of AnMBR (15 kg_{COD}/m³/d) compared to
183 conventional activated sludge (CAS) systems (4 kg_{COD}/m³/d).

184 Recent studies have shown the potential applicability of AnMBR for mainstream DWWT
185 (Maaz et al., 2019; Galib et al., 2016; Pretel et al., 2016). Extensive work on AnMBR has
186 been published at pilot scale to pave the path for its full-scale implementation (Shin and Bae,
187 2018). Nevertheless, membrane fouling remains one of the most challenging issues impeding
188 the development of AnMBRs (Maaz et al., 2019; Saleem et al., 2016), especially with high
189 free biomass concentration widely used in conventional AnMBRs.

190 Membrane fouling is an inevitable phenomenon and conventional AnMBRs mostly make use
191 of biogas sparging (GSP) or crossflow velocity (CFV) to remove (or limit) fouling by
192 promoting turbulences close to the membrane surface (Hu et al., 2007). Total energy
193 requirements of AnMBR with biogas sparging were reported to be from 0.038 to 5.68
194 kWh/m³ (Martin et al., 2011) and crossflow velocity was reported to consume from 3 to 7.3
195 kWh/m³ (Aslam et al., 2017) depending upon CFV and mixed liquor suspended solids
196 (MLSS) of the reactor. It has been reported that fouling mitigation could account for up to
197 70% of total energy consumption in AnMBRs (Shin and Bae, 2018). To design an energy-
198 efficient fouling mitigation technique, many studies were carried out during the last decade
199 understanding fouling behavior (Maaz et al., 2019; Charfi et al., 2017b; Chen et al., 2017a;
200 Xiong et al., 2016; Ding et al., 2015; Chen et al., 2014; Charfi et al., 2012; Herrera-Robledo
201 et al., 2011) and investigating various fouling control strategies (Robles et al., 2018; Shin et
202 al., 2018; Krzeminski et al., 2017; Aslam et al., 2014). Fouling mechanisms in AeMBR
203 (Aerobic Membrane Bioreactor) and AnMBR were compared and were found to be quite
204 different. In AeMBR, adenosine triphosphate (ATP) concentration was 30-fold higher than in
205 AnMBR which leads to higher microbial activity and results in a large fraction of
206 extracellular polymeric substances (EPS) on the membrane surface. Thus, the main
207 contributors to fouling in AeMBR arise from microbial activity during substrate
208 biodegradation. In AnMBR, soluble microbial products (SMP) levels are up to 5 times higher

209 and with higher molecular weights than in AeMBR (i.e; 2526 kDa and 180.1 kDa of
210 carbohydrates detected in the SMP and 630-640 kDa and 0.9 kDa of protein MW detected in
211 SMP for AnMBR and AeMBR respectively). This caused a higher rejection of proteins and
212 carbohydrates in AnMBR which further deposit on the membrane surface thereby resulting in
213 more severe organic fouling and biofouling in AnMBRs (Xiong et al., 2016). It has also been
214 reported that inorganic fouling propensity is higher in AnMBR than AeMBR due to higher
215 carbonate, bicarbonate, ammonia and phosphate concentrations in anaerobic reactors (Lin et
216 al., 2013).

217 It has been established that the fouling in AnMBRs has remained one of the biggest hurdles
218 in positive energy treatment of DWWT (Maaz et al., 2019). Thus, the focus of this review is,
219 particularly on fouling. It aims to present the work that has been done so far in understanding
220 and optimizing fouling mitigation in AnMBRs for domestic wastewater treatment, highlights
221 the different potential technologies in this regard and provides researchers, working in this
222 area, with information that can help in giving them directions for future research work.

223 The paper has been divided in to two major sections, the first will shed light on the current
224 state of the art based on the return of experience and progresses of AnMBR at the pilot-scale
225 for DWWT. The aim of this section is to inform the readers with the basics of fouling
226 mechanism in the AnMBRs, the important definitions and concepts for the understanding of
227 fouling behaviors, factors effecting and fouling control. It will also provide an overview of
228 the latest research trends for fouling mitigation strategies in such systems. In the second
229 section, emerging novel configurations like granular AnMBR (G-AnMBR), AnMBR
230 combined with forward osmosis membrane (FO-AnMBR), entrapped cell-based AnMBR,
231 dynamic AnMBR (AnDMBR) and microbial electrolysis cell AnMBR (MEC-AnMBR) will
232 be discussed in term of removal efficiencies and fouling. These configurations are selected
233 based on their contribution to fouling control. They were designed by researchers to provide

234 solution to the issues of energy intensive fouling control and enhance membrane operation
235 with both technical and economic optimization. Respecting the review's focus on fouling,
236 other innovative techniques that are particularly developed to tackle fouling like quorum
237 quenching and rotation/vibration application are also discussed. Some insight on methane
238 production and potential energy generation are also provided.

239 **2. Current status of operation and fouling in pilot-scale**

240 **AnMBR**

241 The majority of pilot-scale AnMBR systems were designed using commercially available
242 membrane modules and were fed with real or synthetic domestic wastewaters to reflect
243 seasonal and daily variations of the wastewater composition. Data acquired from various
244 pilot-scale AnMBR experiments is crucial to upscale, design and develop full-scale AnMBR.
245 This section reviews the latest outcomes of the pilot-scale AnMBR systems for DWW
246 treatment to extract practical data for the commercial use of AnMBR based plants in the
247 future.

248 **2.1. Configuration models of pilot-scale AnMBRs for fouling control**

249 This section deals with the evaluation of 13 pilot-scale AnMBR studies performed from 2011
250 to 2019 (Table 1). The two-stage reactor was used by 12 pilot-scale AnMBRs, featuring
251 anaerobic reactor with an externally submerged membrane tank (MT). Only one AnMBR
252 system with gas sparging (Config-9) having one stage integrated with an up-flow anaerobic
253 sludge blanket (UASB) combined with a submerged type membrane in the upper portion of
254 the UASB reactor system was reported. In the case of a 2-stage reactor configuration, the
255 membrane is immersed in a separate tank so that intensive shear stress can be applied only on
256 the membrane to control fouling. Moreover, in situ membrane chemical cleaning can be
257 performed in the membrane tank without endangering the whole active biomass. The

258 retentate from the membrane tank is circulated back into the anaerobic reactor to enhance the
259 degradation of organic compounds. In config-12, instead of the continuous stirred tank
260 reactor (CSTR) and separate membrane tank, anaerobic fluidized bed reactor (AFBR) and
261 anaerobic fluidized membrane bioreactor (AFMBR) are used in 2-stages (Config-12; Table-
262 1).

263 The bibliographic study of the 13 AnMBRs (Table-1) shows that three different scouring
264 approaches were used: gas sparging (GSP) (Config-1 to Config-11), particle sparging (PSP)
265 (Config-12) and rotating membrane (RMEM) (Config-13). Most of the membranes were
266 hollow-fiber (HF) submerged membrane except the first one which was a flat sheet (FS)
267 membrane module called GSP-FS (Config-1). AnMBR systems used ultrafiltration (UF)
268 membranes except for GSP-HF_{MF} (Config-6) which featured a MF membrane.

269 Apart from gas sparging, particle sparging and membrane rotation, some additional
270 mechanisms were also employed in different configurations. In Config-1, circulating sludge
271 was used to create additional shear to control membrane fouling. Ventilation and
272 backwashing mechanisms were used in Config-3 and Config-4. Backwashing was used as an
273 anti-fouling mechanism in Config-6 and Config-9. Chemical cleaning was employed for
274 Config-7 and Config-8. Section 2.3 contains a detailed discussion regarding those different
275 anti-fouling strategies.

276 **2.2. Fouling mechanisms in pilot-scale AnMBRs**

277 Membrane fouling is indicated by many factors like increased transmembrane pressure
278 (TMP) (at constant flux), reduced flux (at constant TMP), presence of extracellular polymeric
279 substances (EPS) and soluble microbial products (SMP) in the bulk phase. A significant
280 number of studies are dedicated to understanding EPS and SMP behavior and role in AnMBR
281 fouling (Chen et al., 2017a; Xiong et al., 2016; Ding et al., 2015; Chen et al., 2014; Herrera-

282 Robledo et al., 2011). EPS and SMP play a significant role in membrane fouling due to
283 surface blocking and pore accumulation. SMP which consists mainly of soluble proteins,
284 polysaccharides and humic-like material is defined as an organic matter that can pass through
285 a filter of 0.45 μm and is responsible for adsorption on the surface and within the membrane
286 pores (Chen et al., 2017a). The composition of extracellular polymeric substances (EPS)
287 depends on the process parameters and wastewater composition as well as its origin.
288 However, in general, it consists of insoluble carbohydrates, proteins, lipids and nucleic acid
289 in a highly hydrated gel matrix (Laspidou et al., 2002). EPS contributes mainly to the cake
290 layer fouling due to its ability to flocculate sludge on the membrane surface (Chen et al.,
291 2017a). A study (Liu et al., 2012) explained that the cake formation in such systems was due
292 to higher soluble microbial products (SMP) and higher tightly bound to loosely bound
293 extracellular polymeric substances (EPS) ratio. Pore constriction and blockage results mostly
294 in irreversible fouling but correspond only to 0.9% of total resistance to filtration, hence
295 minimization of cake formation is more strategic than pore fouling in overall fouling
296 mitigation (Chen et al., 2014).

297 Ding et al. (2015) reported that EPS extracted from bulk sludge and cake sludge were
298 responsible for the largest decline in membrane flux. Herrera-Robledo et al. (2011) found that
299 80% of the fouling was caused by EPS and SMP in PVDF membrane tubes. Shin et al. (2014)
300 employed an intermittent membrane relaxation mechanism to control the fouling and drastic
301 rise of TMP.

302 Fouling phenomenon is also influenced by the type of membrane modules in pilot-scale
303 AnMBR. Flat membranes appear to be more sensitive to fouling than hollow fiber
304 membranes. Indeed, it appears that scouring methods are less effective for FS than for HF
305 and a higher fouling rate of 3.33 Pa/s was observed for Config-1, i.e., flat-sheet membrane

306 module (Martinez-Sosa et al., 2011); where a much lower fouling rate of 0-2.5 Pa/s was
307 observed for Config-13, i.e., a hollow fiber membrane module (Martinez-Sosa et al., 2011).

308 Different fouling rates are observed also due to the difference in TMP. TMP of 17.7 kPa and
309 10 kPa were observed for Config-1 and Config-10 respectively indicating higher fouling in
310 Config-1. It is evident from TMP and fouling rate values that Config-1 is more affected by
311 fouling than Config-10 due to the requirement of higher TMP to achieve the same permeate
312 flux. A higher level of fouling rates needs higher energy to reduce it. Config-1 requires
313 higher energy for fouling control (1.28 kWh/m³) when compared to Config-10 (0.23
314 kWh/m³).

315 **2.3. Fouling mitigation strategies in pilot-scale AnMBRs**

316 Three major strategies for fouling mitigation are described below: scouring methods,
317 filtration cycles and chemical cleaning cycles.

318 **2.3.1. Scouring methods**

319 Three methods: biogas sparging (GSP), particle sparging (PSP) and rotating membrane
320 (RMEM) can be used to provide shear stress to mitigate membrane fouling. GSP approach is
321 the most common strategy to control fouling in AnMBR; this technique has been used in 11
322 out of 13 pilot-scale studies referenced in Table 2. The crossflow velocity (CFV) is
323 considered as a key factor for fouling mitigation when sludge recirculation is applied
324 (Skouteris et al., 2012). Almost all the pilot-scale AnMBR systems (except GS-H5)
325 incorporates sludge recirculation in the membrane tank to allow turbulent flow regime close
326 to the membrane surface thereby reducing the thickness of the laminar boundary layer with
327 better mixing of sludge (Lin et al., 2013; Smith et al., 2012). The applied CFV and Gas
328 Sparging Intensity (GSI_m) values were 9.7–94 m/h and 0.15–1.20 N.m³/(m²h), respectively.
329 Config-7 used FeCl₃ (26 mg/L) for flux enhancement. Addition of coagulant results in the

330 reduction of fouling potential by enhancing floc sizes of the colloidal foulants present in the
331 bulk, i.e., improvement of membrane fouling mitigation (Judd, 2011; Holbrook et al., 2004).

332 AnMBR with PSP (Config-13) is known as AFMBR (i.e., anaerobic fluidized membrane
333 bioreactor). In AFMBR, fluidizing granular activated carbon (GAC) acts as the support
334 medium for microorganisms along with playing a role in the scouring of the membrane
335 surface (Kim et al., 2011). AFMBR requires a lower amount of energy and shows lower
336 fouling potential as compared to AnMBR with gas sparging (Aslam et al., 2016; Shoener et
337 al. 2016; Aslam et al. 2014).

338 Rotating membrane sparging is the last fouling control approach employed in Config-13 of
339 pilot-scale AnMBR. This system makes use of the turbulence produced by the rotating
340 membrane module to mitigate the foulant deposition on the membrane surface (Jiang et al.,
341 2012). This technique has recently emerged as an efficient method with higher fouling
342 control and lower energy consumption (Ruigómez et al. 2017; Ruigómez et al. 2016;).

343 **2.3.2. Filtration cycles in AnMBRs**

344 All the above pilot-scale configurations except Config-13 were operated intermittently, i.e.
345 filtration cycles were followed by relaxation cycles with optional cycles of backwashing.
346 Most of the configurations used intermittent cycles of filtration with an integrated
347 backwashing cycle except for the case of Config-12 and Config-7, respectively. Generally,
348 the filtration time with respect to the total time of operation was larger with backwashing
349 (around 79–96 %) than without backwashing (around 80–83 %).

350 **2.3.3. Chemical cleaning cycles**

351 A preventive approach to uphold the membrane permeability is intermittent maintenance
352 chemical cleaning. Only 2 out of 13 experiments used chemical cleaning. In Config-7,
353 maintenance cleaning was performed after every 7 days using a backwashing liquid

354 consisting of 2000 mg/L citric acid at a flux of 32.2 LMH. Config-7 also underwent recovery
355 cleaning by soaking the membrane sequentially (for 16 hours) in the solution of 2000 mg/L
356 of NaOCl and 2000 mg/L of citric acid, respectively. In Config-8, recovery cleaning was
357 performed 7 times (for 4–6 hours) during a period of 1350 days with 1000 mg/L solution of
358 NaOCl at room temperature.

359 **2.4. Removal of organics in pilot-scale AnMBRs**

360 Operating conditions and performances of pilot-scale AnMBR used for DWWT are
361 illustrated in Table 1 and Table 2. It was observed in all 13 studies that COD feed
362 concentrations ranged from 198 mg/L to 1460 mg/L and HRT was in the range of 2.20–33
363 hours. For WW having higher concentrations of COD in the influent (i.e., COD > 500 mg/L),
364 HRT was generally higher than 10 hours. The maximum HRT of 33 hours was observed for
365 Config-13 while the minimum HRT of 2.2 hours was observed for Config-6. SRT for all
366 AnMBR configurations ranged from 6 days to infinite value (no waste of biomass, except for
367 sludge sampling). The maximum SRT of infinite days was observed for Config-8 and
368 minimum SRT of 6.2 days was observed for Config-12. On the other hand, the maximum
369 Organic Loading Rate (OLR) range of 3.77–4.97 kg_{COD}/(m³.d) was observed for Config-10
370 while Config-3 showed the minimum OLR range of 0.3–1.1 kg_{COD}/(m³.d).

371 The majority of the AnMBR systems were conducted under room temperature conditions
372 (i.e., 17–35 °C) and Config-10 was operated over a broad range of temperatures (from 9 to 30
373 °C). The operating permeation flux was within 4.1–17 LMH; the highest flux of 17 LMH was
374 achieved after the incorporation of 26 mg/L of FeCl₃ to Config-7 and Config-10. The
375 concentrations of MLSS ranged from 600 to 32000 mg/L. It must be noticed that MLSS was
376 higher in GSP systems (around 7000–32000 mg/L) than in PS systems (around 600–12000
377 mg/L).

378 All the configurations exhibited COD removal efficiencies greater than 85%. Config-12
379 shows a high COD removal efficiency (more than 90%) even if this process was conducted in
380 psychrophilic conditions (9–11 °C). Introduction of the flux enhancer (e.g., FeCl₃) improved
381 COD removal efficiency (79.9% to 93.7%) for Config-7 and Config-10 due to aggregation of
382 colloidal organics followed by their rejection by the membrane.

383 **2.5. Energy requirements in the pilot-scale AnMBRs for fouling** 384 **mitigation**

385 An increasing crossflow velocity allows reducing membrane fouling but requires more
386 energy consumption. For example, increasing crossflow velocity from 1 to 2 m/s increased
387 permeate flux by about 20 %, but also the energy requirement by about 60 % (Bourgeois et
388 al., 2001). Besides, the high shear rate can provide a negative effect on microbial activities in
389 AnMBR due to the disaggregation of microbial flocs. The data of energy consumption along
390 with the corresponding transmembrane pressure for all the AnMBR configurations (11 GSP
391 AnMBRs, one PSP AnMBR and one RMEM AnMBR) is given in Table 3. It is evident from
392 Table 3 that the energy requirement for fouling control in AnMBRs is the most significant
393 constituent of the system, as it constitutes more than 75% of the total energy intake (Smith et
394 al., 2014; Lin et al., 2011). The energy requirement for fouling mitigation mainly relies on the
395 scouring method (Pretel et al., 2014). The estimated energy demand in the GSP AnMBR
396 system varies between 0.05 kWh/m³ and 1.66 kWh/m³ with an average energy of around 0.39
397 kWh/m³. Among all the GSP AnMBRs, the highest energy demand was observed for the FS
398 membrane (Config-1). The average energy demand for Config-1 was 1.66 kWh/m³ having a
399 peak GSI_m value of 1.2 N m³/ (m².h) with a comparatively lower critical flux of 7.0 LMH
400 (Krzeminski et al., 2012; Verrecht et al., 2008). The average energy requirement for GSP
401 AnMBRs with HF membranes (Config-2 to Config-10) was 0.28 kWh/m³. However, GSP

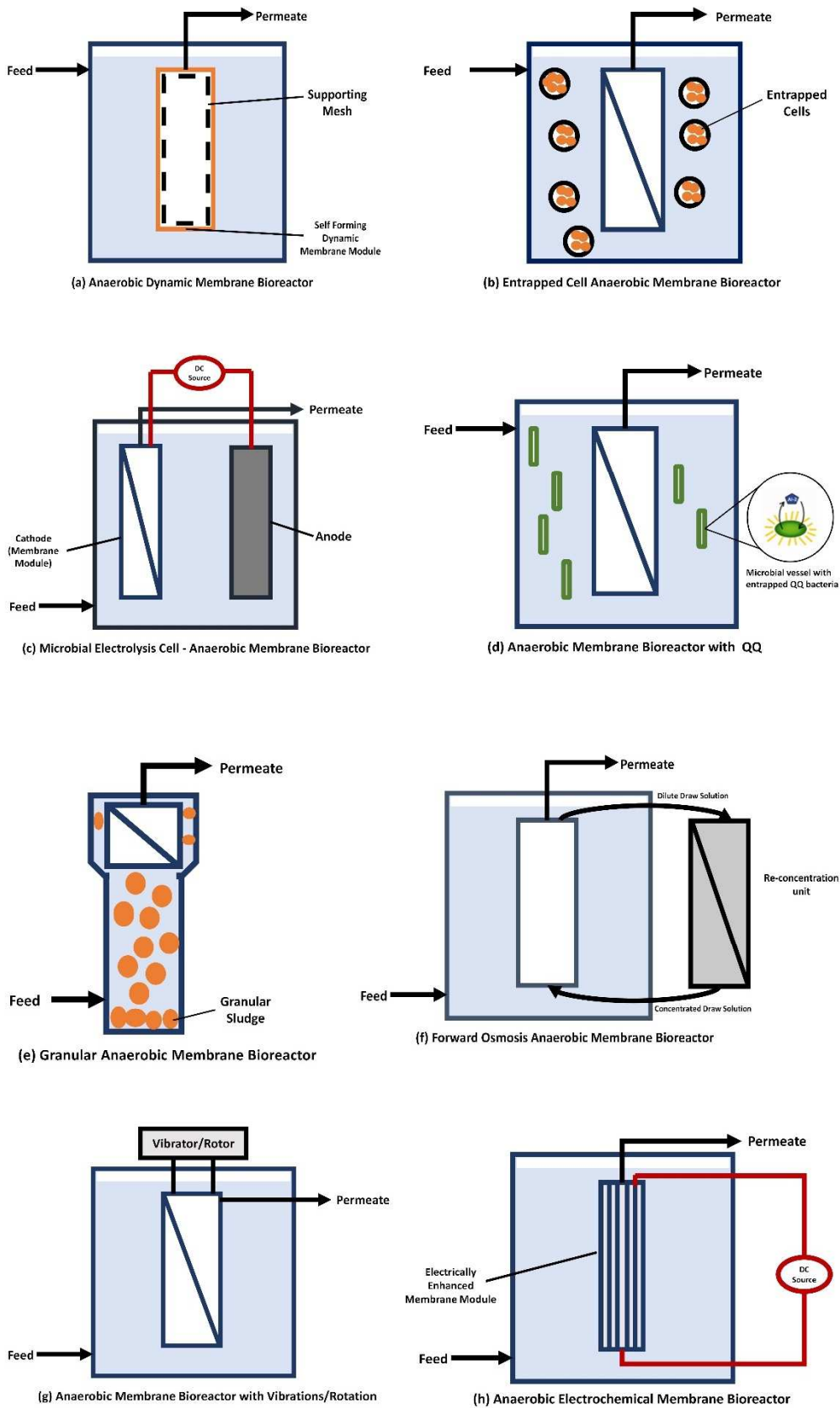
402 AnMBRs still requires roughly 65% less energy than AeMBRs (0.70–0.90 kWh/m³)
403 (Krzeminski et al., 2012).

404 The energy requirement for a GSP AnMBR depends on the flux conditions and GSI_m. HF
405 AnMBRs require lower GSI_m than FS modules. Amongst hollow fiber AnMBRs, Config-7,
406 Config-9 and Config-10 required the lowest energies due to lower GSI_m values of around
407 0.15-0.32 N.m³/(m².h). For Config-7 and Config-10, lower GSI_m was achieved by the
408 addition of coagulant (i.e., flux enhancer). On the contrary, lower GSI_m in Config-9 is due to
409 lower solid concentration in the membrane containing tank coupled with recirculation of
410 liquid between the membrane tank and the biological reactor.

411 The relationship between energy requirement and flux is illustrated by drawing a comparison
412 of flux, TMP and energy demands for Config-3 and Config-4 operated under the same GSI_m.
413 The increment of flux from 10 LMH (Config-3) to 13.3 LMH (Config-4) at the same GSI_m
414 resulted in lower energy demand (0.164 kWh/m³) for Config-4 as compared to Config-3
415 (0.198 kWh/m³). Similarly, the specific energy demand of PSP AnMBR can also be reduced
416 by increasing the flux. The energy demand in the PSP AnMBR (Config-10) for GAC
417 fluidization was reported to be 0.102 kWh/m³. McCarty et al. (2011) assessed the decrease in
418 energy requirement to be 0.070 kWh/m³ for PSP AnMBR. The estimated energy demand for
419 a staged anaerobic fluidized AnMBR (Config-10) is 0.23 kWh/m³ with a flux of 10 LMH
420 and membrane rotation velocity of 100 rpm.

421 **3. Novel AnMBRs for fouling mitigation**

422 This section has designed to demonstrate (1) novel AnMBRs configurations and their impact
423 on fouling; (2) impact of specialized fouling mitigation techniques on total fouling control in
424 AnMBR for DWWT. Figure 1 shows the schematics of different novel configurations (a, c, e
425 and f) of AnMBRs and specialized fouling mitigation strategies (b, d, g and h).



426

427

428

429

Figure 1 Schematics of different AnMBR schemes. (a) Dynamic AnMBR (b) Entrapped Cell AnMBR (c) MEC-AnMBR (d) AnMBR with QQ (e) G-AnMBR (f) FO-AnMBR (g) AnMBR with vibration/rotation (h) Electrochemical AnMBR

430 **3.1. Granular-AnMBR**

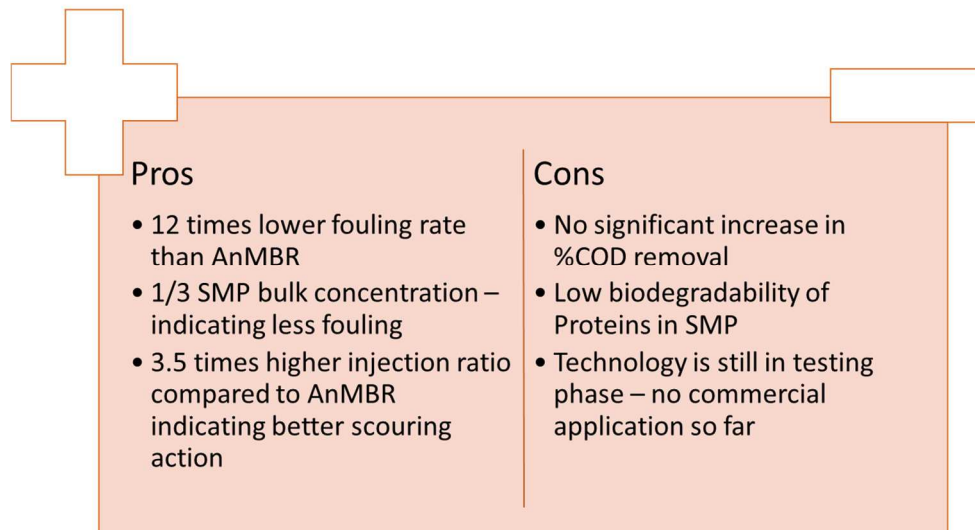
431 Coupling of membrane separation with anaerobic granular sludge (AnGS) reactors constitutes
432 an interesting perspective. The most promising feature in G-AnMBR is the way to control
433 membrane fouling. The structure of AnGS is not only justified for decantation but also to
434 limit fouling phenomena. AnGS recirculation promotes mechanical scouring actions
435 alongside the membrane surface and contributes to reduce membrane fouling. Fluidized
436 AnGS comes into physical contact with the membrane surface, and their physical movement
437 helps to reduce membrane fouling at a relatively low energy cost (Kim et al., 2011).
438 Furthermore, when AnGS are used as fluidized media, the biological kinetics rate increases
439 leading to a reduction of colloidal and dissolved organic matter (DOM), further decreasing
440 irreversible fouling due to this DOM and increasing treatment stability and efficiency (Aslam
441 et al., 2014). However, very little knowledge is available regarding the mechanisms of the
442 mechanical cleaning process and fouling mitigation during DWWT by AnGS in G-AnMBR.
443 Although G-AnMBR has a great potential to achieve energy-positive domestic wastewater
444 treatment, the extent of fouling and energy consumption in the G-AnMBR can be strongly
445 affected by the biological and physio-chemical properties of the AnGS. There are still several
446 research questions to be resolved to optimize the selection of granular sludge. Besides, the
447 energy requirement for fluidization in the G-AnMBR is closely related to the packing ratio of
448 AnGS and their physical properties such as nature, size and shape. A better understanding of
449 the links between AnGS characteristics, operating conditions (characteristic of the feed
450 (DOM, mass loading rate), hydrodynamics, solid and liquid residence time) and fouling
451 mitigation efficiencies (TMP, resistances), are thus needed (Aslam et al., 2017; Choo et al.,
452 1998). The following section will discuss studies on G-AnMBR in detail and will also present
453 a comparison with conventional AnMBR.

454 3.1.1. G-AnMBR v/s Conventional AnMBR

455 G-AnMBR combines the benefits of granulation and membrane separation and overcome
456 drawbacks associated with conventional anaerobic sludge bioreactor like long startup time,
457 high operating temperature, poor settling, poor nutrient removal and need for post-treatment
458 (Chen et al., 2016). A study (Martin-Garcia et al., 2011) comparing the performance of G-
459 AnMBR versus conventional flocculated AnMBR during 250 days showed almost similar
460 COD removal in both the cases (84% in AnMBR and 86% in G-AnMBR). However, a great
461 difference in MLSS and SMP bulk concentrations (598 ± 150 mgCOD/L for AnMBR and
462 198 ± 73 mgCOD/L for G-AnMBR) was found, indicating less fouling propensity in G-
463 AnMBR. Protein to carbohydrate (P/C) ratio in SMP was found higher for G-AnMBR (2.8 in
464 G-AnMBR v/s 2.3 for AnMBR), probably due to infinite SRT compared to AnMBR which
465 resulted in accumulation of proteins in SMP and thus indicating low biodegradability of
466 proteins in case of G-AnMBR.

467 Superficial liquid velocity (V_L) induced by gas velocity (V_G) (nitrogen in this case) was much
468 higher in the case of G-AnMBR for similar V_G of 0.02 m/s, (i.e. had V_L of 0.26 and 0.09 m/s
469 for G-AnMBR and AnMBR respectively). Thus, injection ratio ($IR = V_G / (V_G + V_L)$) was
470 much lower for G-AnMBR (0.07 to 0.2) compared to AnMBR (0.26 to 0.71), indicating
471 better scouring action in the case of G-AnMBR. Interestingly, for the same flux of 11 to 12
472 LMH, the fouling rate in G-AnMBR was only 1.67-3.33 Pa/s compared to a much higher
473 fouling rate of 13.33 to 41.67 Pa/s in AnMBR. Also, using fluid pumping to generate
474 crossflow velocity (CFV) for the same increase in CFV (0.4 to 2m/s), a greater increase of
475 flux was observed in G-AnMBR (4 to 41 LMH) compared to AnMBR (4 to 19 LMH)
476 indicating lesser CFV requirements for suppression of cake enhanced concentration
477 polarization in case of G-AnMBR. Even in the case of an immersed HF module, gas
478 (nitrogen) demand was 50% less in G-AnMBR as compared to AnMBR (Martin-Garcia et al.,

479 2011). These low scouring requirements and less fouling make G-AnMBR a potential
480 solution for fouling and energy-related issues in AnMBR for DWWT. Figure 2 summarizes
481 the pros and cons of G-AnMBR.



482

483

Figure 2 Pros and Cons of G-AnMBR compared to AnMBR

484

3.1.2. Effect of configuration on fouling in G-AnMBR

485

When internally submerged (SG-AnMBR) and external (EG-AnMBR) membrane configurations were compared, it was found that with approximately the same COD removal efficiencies SG- AnMBR was more prone to fouling than EG-AnMBR (Chen et al., 2017b).

488

It was explained that the direct addition of membrane in the reactor results in almost complete colloidal flocs retention resulting in their accumulation and thus enhancement in the growth of bulking sludge which is dispersed and has poor immobilization. This phenomenon

491

dominates over the growth of granular sludge and thus resulted in low biomass growth rate (0.02 gMLSS/d v/s 0.05 gMLSS/d), settling velocity (12.1-17.2 m/h v/s 14.1-28.5 m/h) and

493

zeta-potential (-19.1 v/s -13.1) in SG-AnMBR compared to EG-AnMBR. Accumulation of fine and small flocs in SG-AnMBR also accounted for higher MLSS (180.2 ± 9.12 mg/L)

495

which in turn was responsible for higher EPS and SMP production thus more fouling.

496

Moreover, protein-based EPS in the cake layer was higher for SG-AnMBR (11.7 mg/g of

497 cake layer) than EG-AnMBR (8.5 mg/g of cake layer), indicating a stickier cake layer
498 resulting in more severe fouling and permeate flux drop. The same was observed for SMP
499 (18.6 v/s 10.2 mg/g of cake layer) resulting in more adhesion of sludge on the membrane
500 surface. This could cause irreversible fouling by forming a thin gel layer at the membrane
501 surface (Chen et al., 2017b). Biopolymers were found to be major contributors in organic
502 fouling with a noticeable difference of concentration in both configurations. Reported values
503 in SG-AnMBR and EG-AnMBR were 14.6 and 6.8 mg/L, respectively. Their high
504 concentration might result in the build-up of a hydrophilic layer by biopolymers attachment
505 on the membrane surface. Building blocks (BB), low molecular weight (LMW) neutrals and
506 acidic compounds can also enhance biopolymer production and attachment to the membrane
507 surface thereby contributing to the increased fouling. Their concentrations were also higher
508 for SG-AnMBR (6.3 mg/L BB and 9.7 mg/L LMW) compared to EG-AnMBR (4.6 mg/L BB
509 and 5.9 mg/L LMW) (Chen et al., 2017b).

510 **3.1.3. Effect of gas sparging regime on performance and energy demand in G-** 511 **AnMBR**

512 To evaluate the effect of the GSP regime on performance and energy demand of G-AnMBR,
513 (Wang et al., 2018a), a study was performed with pilot-scale SG-AnMBR treating DWW and
514 operating it under three different GSP conditions that were: (1) continuous filtration and GSP,
515 (2) continuous filtration with intermittent GSP and (3) intermittent filtration and GSP in
516 pseudo dead-end filtration (filtration cycle of nine minutes without GSP followed by one
517 minute of GSP and membrane relaxation). HRT was kept at 8 hours and the temperature of
518 the influent was around 16.3 ± 3.7 °C. 40 % bed expansion was achieved by maintaining an
519 up-flow velocity of 0.8-0.9 m/h. During the 400 days trial, there was no withdrawal of
520 biomass. Intermittent filtration and sparging in pseudo dead-end filtration was found to be the
521 most suitable configuration among all three that had provided sustainable fouling rates with

522 minimum energy requirements (0.133 kWh/m^3 with net SGD of $0.2 \text{ m}^3/(\text{m}^2\cdot\text{h})$). The authors
523 explained that in the case of dead-end filtration, particulate materials, colloids and soluble
524 materials deposited simultaneously compared to continuous GSP where induced shear stress
525 close to the membrane surface caused particle size segregation resulting in preferential
526 migration of colloids towards the membrane surface. This deposition resulted in a
527 heterogenous cake layer. However, this is only possible when solid concentration is low
528 enough to allow limited cake deposition in a specific filtration cycle since TMP and filtration
529 time influence cake compressibility. At 13.5 LMH, SGD per unit permeate of $14.8 \text{ m}^3/\text{m}^3$ was
530 similar to that in a plant scale AeMBR treating municipal waste ($14\text{-}30 \text{ m}^3/\text{m}^3$) despite more
531 complex fouling behaviors on anaerobic treatment.

532 **3.1.4. Sponge assisted G-AnMBR**

533 To minimize the fouling rate in SG-AnMBR, the effect of polyurethane sponge incorporation
534 was studied (Chen et al., 2017c). Decreasing the fouling rate in SG-AnMBR will make it
535 superior to external configuration since it has lower capital and operational costs. Sponges act
536 as media to provide a high specific area for the growth of biomass by increasing the
537 flocculation of sludge due to porosity and resistance against hydrolysis. Sponge assisted G-
538 AnMBR contains about 84 % of total granular sludge and this is about two times higher than
539 conventional granular bioreactor (about 42.5 %) due to the immobilization of fine particles on
540 or inside the pores of the sponge. EPS plays an important role in granular formation by
541 allowing cell integration and helping to keep sludge intact. The average fouling rate in
542 sponge assisted G-AnMBR was about 0.006 Pa/s which is lower than that of conventional G-
543 AnMBR (0.014 Pa/s). This difference in fouling rates can be explained by SMP and EPS
544 concentrations in mixed liquor as well as the cake layer. In conventional G-AnMBR, granules
545 and floc breakage increase SMP concentration ($47.3\pm 7.6 \text{ mg/L}$) and EPS ($24.5\pm 11 \text{ mg/L}$). In
546 contrast, sponge assisted G-AnMBR exhibits relatively low SMP and EPS concentrations of

547 15.9±3.5 mg/L and 17±6.2 mg/L, respectively. Lower SMP and EPS concentrations are due
548 to adsorption of sludge on the sponge and the majority of biodegradation occurs inside
549 granules and sponge-attached biomass. Reduced free fine flocs and colloids in sponge
550 assisted G-AnMBR resulted in a less dense fouling cake layer than that observed in
551 conventional G-AnMBR. Overall fouling resistance is reduced since cake layer fouling is
552 dominant in AnMBR. Moreover, cell lysis in conventional G-AnMBR results in higher
553 protein EPS (12.1 mg/g of cake layer in conventional v/s 10.7 mg/g of cake layer in sponge
554 assisted) and protein SMP (8.2 mg/g of cake layer in conventional v/s 5.6 mg/g of cake layer
555 in sponge assisted) which forms stickier cake and thus contributes more to fouling filtration
556 resistance. In addition to less fouling, sponge assisted G-AnMBR also provides the benefit of
557 a 17 % higher methane yield. Another configuration that has employed sponges and that was
558 designed for fouling control was sponge assisted AnMBR with rotary disk (Kim et al., 2014).
559 It utilized polyurethane sponge to support microbial growth and the disk rotates parallel to the
560 surface of 2 flat sheet submerged membrane for fouling control. 96% COD removal and
561 150±29 mL CH₄/g COD methane yield were obtained by performing experiments using a 50
562 % volume fraction of sponge, 6 hours HRT, 11 LMH flux and 70 rpm rotation speed of the
563 disk. TMP rise rate of 0.15 Pa/s was observed compared to 5 Pa/s without rotation indicating
564 effective fouling mitigation. This was attributed to high collision energy between sponge and
565 membrane surface, reducing cake enhanced concentration polarization. Operational
566 electricity consumption was ten times lower by combining rotation and sponge media than
567 the energy produced by methane combustion. As a result, the operation of this hybrid
568 AnMBR provided net positive energy of 0.04 kWh/m³. This study demonstrated a potential
569 configuration for the net positive energy operation of AnMBR for DWWT. However, a
570 detailed study regarding fouling behaviors under different operational conditions and floating
571 media is necessary before scale-up.

572 **3.2. Entrapped cell AnMBR**

573 Cell entrapment makes use of a polymer matrix to artificially entrap cells providing increases
574 resistance to washout. Juntawang et al. (2017) used phosphorylated polyvinyl alcohol for cell
575 entrapment in AnMBR and compared it with conventional suspended cell AnMBR. Both
576 units showed the same COD removal efficiencies (approximately 84 % COD removal) which
577 indicates that cell entrapment has no negative impact on treatment. Fouling resistance in
578 entrapped cell based AnMBR was found to be 0.32×10^6 1/m for pore blockage and 1.06×10^6
579 1/m for the cake layer. These are less than the suspended one (2.54×10^6 1/m for pore
580 blockage and 1.69×10^6 1/m for cake layer) indicating less fouling propensity. Cell entrapment
581 results in lower EPS and SMP concentration as well as larger particle size. Conventional
582 AnMBR has much higher pore blockage resistance which indicates more potential for
583 irreversible fouling and thus would need more intensive chemical cleaning. However,
584 bacterial communities in both the cases were similar except bacteroidetes colonies which
585 were more abundant in suspended cell AnMBR than in entrapped cell AnMBR. The
586 formation of these colonies is favored in the presence of proteinaceous EPS and thus high
587 protein to carbohydrate ratio of EPS. Methane yields in both cases were almost similar i.e.
588 0.23 L/d for entrapped cell bases AnMBR and 0.28 L/d for the suspended one.

589 In 2019, Juntawang et al. (2019) have used the entrapment technique in FO-AnMBR.
590 Polyvinyl acetate (PVA) based entrapped cells were used in side-stream configuration with
591 thin-film composite (TFC) FO membrane to treat domestic wastewater having initial soluble
592 COD of 542 mg/L. Two draw solutions namely NaCl (1.5M) and $(\text{NH}_4)_2\text{SO}_4$ (1M) were
593 tested. In the case of entrapped cells, flux decline rates were 0.042 and 0.049 LMH/day for
594 FO-AnMBRs using NaCl and $(\text{NH}_4)_2\text{SO}_4$ as draw solutions, respectively. Whereas, for
595 suspended cell FO-AnMBR they were 0.057 and 0.074 LMH/day, respectively. Additionally,
596 EPS was 35% and 13% less and SMP was 65% and 68% less in entrapped cell FO-AnMBR

597 using NaCl and $(\text{NH}_4)_2\text{SO}_4$ as draw solutions, respectively. This could be explained by the
598 fact that entrapment keeps the cell activity restricted, and thus control the formation of EPS
599 and SMP. In addition, it might also keep EPS and SMP trapped in, suggesting that fouling
600 potential should be higher with suspended cells than entrapped cells. Entrapped cell-based
601 technologies could be a step forward in terms of fouling mitigation. As seen, they provide
602 better fouling mitigation than conventional AnMBR. More research in this area is needed to
603 conduct energy and cost comparisons so that the technique can be further developed.

604 **3.3. Dynamic AnMBR**

605 In the recent years, anaerobic dynamic membrane bioreactors (AnDMBR) have been
606 investigated as a sustainable solution to wastewater treatment due to their low cost of the
607 membrane, reasonable treatment efficiency (providing 60-90% COD removal and 90-100%
608 turbidity and suspended solids removal) and less fouling ($0.6 \times 10^9 \text{ m}^{-1}/\text{h}$ rate of increase of
609 fouling resistance compared to $40 \times 10^9 \text{ m}^{-1}/\text{h}$ in AnMBRs) (Hu et al., 2018a). Dynamic
610 membrane (DM) bioreactors make use of cheap materials like meshes or fiber cloth as
611 support on which the cake layer is formed instead of expensive ultrafiltration or
612 microfiltration membranes. This cake layer acts as an additional or secondary membrane
613 (dynamic membrane layer) due to its capability of rejecting pollutants such as colloidal
614 materials, microbial cells and organics. Although DM was reported firstly by workers of Oak
615 Ridge National Laboratories in 1965, its application in AnMBR is relatively new and less
616 developed. (Alepu et al., 2016). This section aims at reviewing the existing literature on
617 AnDMBR and how they are useful in resolving the fouling issues for domestic wastewater
618 treatment.

619 **3.3.1. DM layer formation mechanism in AnDMBR**

620 A study (Zhang et al., 2010) proposed a three-step formation mechanism that involves a
621 separation layer formation stage, stage of stable growth and finally a fouling stage. This

622 mechanism was confirmed by other studies as well (Hu et al., 2018b; Siddiqui et al., 2018;
623 Alepu et al., 2016; Alibardi et al., 2016; Ersahin et al., 2016; Zhang et al., 2011). The time
624 required for a stable DM layer formation depends on the operation mode of the reactor. In
625 gravity-driven mode, which allows continuous extraction of effluent without relaxation, this
626 time is about 40-100 minutes whereas in the pressure-driven mode it is about 10-25 days.
627 Operating with intermittent permeate production leads to longer stabilization time both in
628 pressure-driven mode (approximately 50 days) and gravity-driven mode (7 days) (Hu et al.,
629 2018a) compared to the continuous operation.

630 **3.3.2. Submerged versus external dynamic AnMBR**

631 Membrane configuration plays a very significant role in defining performance efficiency as
632 well as fouling propensity in AnDMBR. Submerged AnDMBR was found to be slightly
633 better in terms of removal efficiency on COD and turbidity (99.5 and 99.7 %) than external
634 configuration (Ersahin et al., 2017). The authors also found out that the time required to form
635 a stable DM layer in submerged configuration was only 10 days while it was 20 days in
636 external configuration at the same permeate flux of 2.2 LMH. The DM layer was less stable
637 in the external dynamic membrane due to the high shear rate which affected the system
638 performance. These results indicate that submerged configuration is more appropriate than
639 the external configuration for applications that require smaller startup time and a more stable
640 DM layer. It was also mentioned that increased shear stress in the external case disturbed the
641 balance of the microbial ecosystem and reduced the methane formation thus providing a
642 negative impact on the overall energy balance of the system. This was proved by the fact that
643 the submerged configuration had an average methane flow of 2.4 L/days whereas the external
644 one had 1.9 L/days. However, it was also seen that the submerged configuration has higher
645 filtration resistance (10.2×10^{16} 1/m) and TMP (68.0 kPa) than the external one with 7.4×10^{16}
646 1/m resistance and 38.0 kPa TMP (Ersahin et al., 2017). Higher resistance in submerged

647 dynamic AnMBR was probably caused by the formation of a thick DM layer. External
648 recirculation has an additional scouring effect on the membrane. Differences in performance
649 efficiencies were not too high. To understand which configuration is better for full-scale
650 implementation, it would be important to establish complete energy and economical balances.

651 **3.3.3. Effect of operating conditions in AnDMBR**

652 Operating conditions have a significant effect on DM formation, performance and fouling in
653 AnDMBR.

654 **3.3.3.1. Effect of flux**

655 Higher operating fluxes are required in AnDMBR operations to reduce HRT and thus capital
656 cost and footprint. It was observed that higher flux led to a faster formation of the DM layer.
657 However, the time required for stable operating was reduced from 10 to 5 days as flux
658 increased from 50 to 150 LMH. Higher flux resulted in a faster adsorption rate of suspended
659 solids on the membrane surface (Wang et al., 2018). However, as for other membrane
660 processes, higher fluxes can result in more severe fouling; Other studies observed that higher
661 initial flux causes the higher increase of TMP (Siddiqui et al., 2018; Quek et al., 2017;
662 Saleem et al., 2016; Chu et al., 2014).

663 **3.3.3.2. Effect of organic load and sludge recycling**

664 Hu et al., (2018b) studied the effect of organic load and sludge recycling on the performance
665 of a flat-sheet AnDMBR at 20 °C and a short HRT of 8 hours. In both cases, without sludge
666 recycling (CFV=0.24 m/h) and with sludge recycling (CFV=0.83 m/h), when organic loading
667 rate (OLR) was increased from 0.88 kg_{COD}/(m³.d) to 3.01 kg_{COD}/(m³.d) an increase in COD
668 removal efficiency (approximately 23 % increase) as well as methane yield (approximately 5
669 times increase) were observed. Higher COD removal was attributed to higher retention of
670 organic compounds by a thicker DM layer. However, when OLR was increased, by adding
671 synthetic wastewater, the availability of organic matter to bacteria was increased thus

672 allowing to produce more methane. With sludge recycling, CFV could be increased but it
673 impacted the COD removal negatively. Similar results were observed by (Siddiqui et al.,
674 2018) where an increase of CFV from 54 m/h to 90 m/h s increased turbidity in the permeate
675 (from 10 to 17 NTU). Higher CFV has reduced the thickness of the DM layer, allowing
676 particulate matter to pass through the membrane, which has led to lower permeate quality.
677 The authors also observed that when the organic load was increased, the filtration properties
678 of the membrane deteriorated. TMP did not exceed 15 kPa throughout the operational period
679 when OLR was 0.88 kg_{COD}/(m³.d), but it rose quickly to 20kPa within 20 d of operation for
680 OLR of 1.5 kg_{COD}/(m³.d). For the OLR of 3.01 kg_{COD}/(m³.d), TMP was over 15 kPa in less
681 than 20 d. This behavior could be explained by the fact that more biomass is accumulated in
682 the DM layer at higher OLR.

683 The thickness of the DM layer with sludge recycling was less than without recycling (0.54-
684 0.95 mm compared to 0.76-1.27mm without recycling) due to improved back transport by
685 increased CFV. However, TMP increased faster (15-18 kPa with OLR of 0.88 kg_{COD}/(m³.d))
686 because of sludge structure modification during recirculation. Sludge recycling promoted the
687 formation of fines and colloids, which may have accelerated pore blockage. Moreover, higher
688 amounts of EPS and SMP were observed with sludge recycling (27.5 mg/g MLSS total EPS
689 and 2.67 mg/g MLSS total SMP) compared to without sludge recycling where 13.58 mg/g
690 MLSS total EPS and 1.06 mg/g MLSS total SMP was observed. They were responsible for
691 the higher fouling rate in the case of sludge recycling.

692 **3.3.3.3. Effect of operating time**

693 Operating time or filtration period can have a significant impact on the fouling rate in
694 AnDMBR. It was observed that increasing filtration duration from 60 minutes to 720 minutes
695 increased DM thickness from 2.29 mm to almost 3 mm. This results in irreversible fouling
696 that could not be recovered by backwashing Moreover, the total amount of EPS increased

697 from 28 mg/g VSS to 42 mg/g VSS and total SMP increased from 4 mg/g VSS to 6.5 mg/g
698 VSS as the operation time increased from 60 to 720 minutes (Siddiqui et al., 2018).

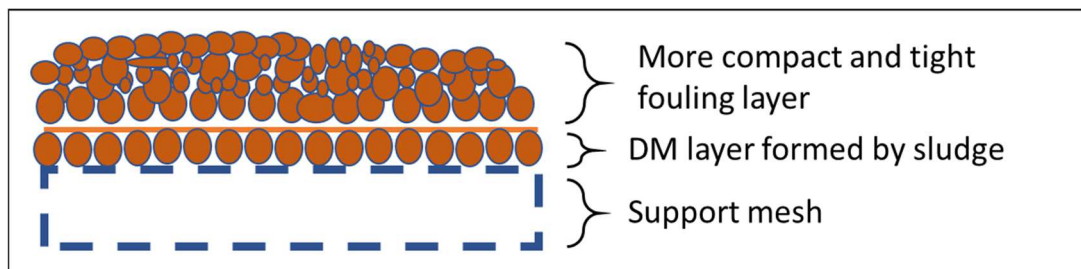
699 **3.3.3.4. Effect of mesh pore size**

700 Mesh size from 10 μm to 200 μm was tested in AnDMBR studies. It can be observed (Table
701 4), that an increase in mesh pore size improves the flux due to reduced filtration resistance.
702 However, it affects the removal efficiency negatively by allowing more passage of solids
703 through mesh pores than UF/MF membranes with much smaller pore sizes. Thus, a trade-off
704 exists between permeate flux and removal efficiency. However, the difference in COD
705 removal efficiency is not significant whereas with larger pore size (46 μm pore size
706 compared to 28 μm) filtration time can be increased up to four times indicating that smaller
707 pore sizes are more prone to fouling (Quek et al., 2017). Moreover, meshes with larger pore
708 sizes are cheaper than smaller pore size ones (Alibardi et al., 2016).

709 **3.3.4. Fouling mechanism in AnDMBR**

710 Fouling has a different meaning for AnDMBRs. Initial accumulation of material on the mesh
711 is the desired DM formation and after DM formation, subsequent deposition that leads to
712 increased resistance to filtration is regarded as fouling (Chu et al., 2014). In one study (Wang
713 et al., 2018) the membrane fouling mechanism for self-forming AnDMBR at 25 °C with
714 polyamide nylon mesh (150 μm pore size) supported by a hollow cylinder was described. The
715 author experienced a three-stage fouling mechanism in AnDMBR operating at a flux of 100
716 LMH. At the first stage, a decrease in resistance was observed. This was due to the increase
717 in membrane hydrophilicity. Hydrophilicity reduces the adsorption of pollutants on the
718 membrane surface. In the second stage, the resistance was rather stable due to the low content
719 of EPS in the system. Finally, in the third stage, resistance increased sharply indicating
720 blockage of membrane pores and enhanced compactness of cake. Zhang et al., (2011)
721 observed membrane foulants in AnDMBR and observed a two-layered structure with an inner

722 layer tightly bonded to the mesh surface and an outer layer loosely bonded to the inner layer.
723 SEM analysis showed that the cake layer developed during the first stage had larger pores
724 and loosely packed sludge flocs. As the stages process, cake compactness has started to
725 increase resulting in a very compact cake layer in the third stage. A similar observation was
726 made by another study (Sun et al., 2018). It is assumed that solid accumulating varies in size,
727 initial coarse particles get deposited but as the DM layer formed, the deposition of small
728 particles leads to a denser cake (Figure 3). Moreover, EPS, polysaccharides, proteins and
729 total cells (that are responsible for fouling in AnMBRs) increased in content as the stages
730 proceed. It was also found (Ersahin et al., 2016) that the average amount of SMP, EPS and
731 EPS P/C ratio of the DM layer was 21.5, 5.8 and 1.9 times (respectively) more than the bulk
732 sludge indicating more resistance and stickier cake.



733

734 *Figure 3 Foulant layer distribution in AnDMBR*

735 **3.3.5. Fouling mitigation in AnDMBR**

736 AnDMBR has provided a cheaper alternative to expensive MF/UF membranes for AnMBRs.
737 The buildup of cake is useful for AnDMBRs but beyond a certain level, it is regarded as
738 fouling and must be controlled to have a long and stable operation. Fouling mitigation
739 techniques like CFV, biogas sparging, back flushing and relaxation can serve the purpose.
740 CFV could help in prolonging the AnDMBR operation however once the cake layer is
741 developed application of large CFV, only has a short-term impact on fouling mitigation. It
742 reduced the TMP value to half (from above 20 kPa to below 10 kPa) when CFV increased
743 from 1 to 5 m/h (Alibardi et al., 2014) but this effect did not last for long and a sharp increase

744 in TMP was observed again after a short time. Moreover, high CFV could modify sludge
745 resulting in a negative impact on filterability as well as biological activity (Hu et al., 2018b).

746 Some studies employed GSP as fouling control in AnDMBR (Li et al., 2017; Yang et al.,
747 2017; Li et al., 2016). Application of biogas sparging (at a rate of 1 L/min) decreased foulants
748 accumulation (38 days to reach maximum TMP with biogas sparging compared to 15 days
749 without) on the mesh surface and offered a less rapid increase of TMP compared to the
750 operation without biogas sparging. This indicates that biogas sparging can effectively scour
751 the foulant layer in DM membranes and increase the operation time. A similar observation
752 was made by Yang et al., (2017) that used N₂ sparging. However, it is important to control
753 the sparging rate. Too much sparging can disturb the DM layer and affect the performance of
754 AnDMBR. Compared to conventional AnMBR less sparging rate is required in AnDMBR as
755 removal of foulants from mesh is easier than MF/UF (Li et al., 2016).

756 As AnDMBR makes use of the cake layer for filtration with comparatively cheap mesh
757 supports which can be easily cleaned and the cake layer can be reformed, not much attention
758 is given to in situ fouling control in AnDMBR. Hence there is a need to investigate in further
759 detail the effect of in situ fouling control methods on performance as well as the lifetime of
760 AnDMBRs. It is also needed to carry out economic and energy calculations on AnDMBR
761 with and without in situ fouling control to establish comparisons with conventional AnMBRs
762 and evaluate the feasibility of AnDMBRs for the long term and large-scale applications.

763 **3.4. Forward Osmosis AnMBR (FO-AnMBR)**

764 **3.4.1. Configuration and working principle of FO-AnMBR**

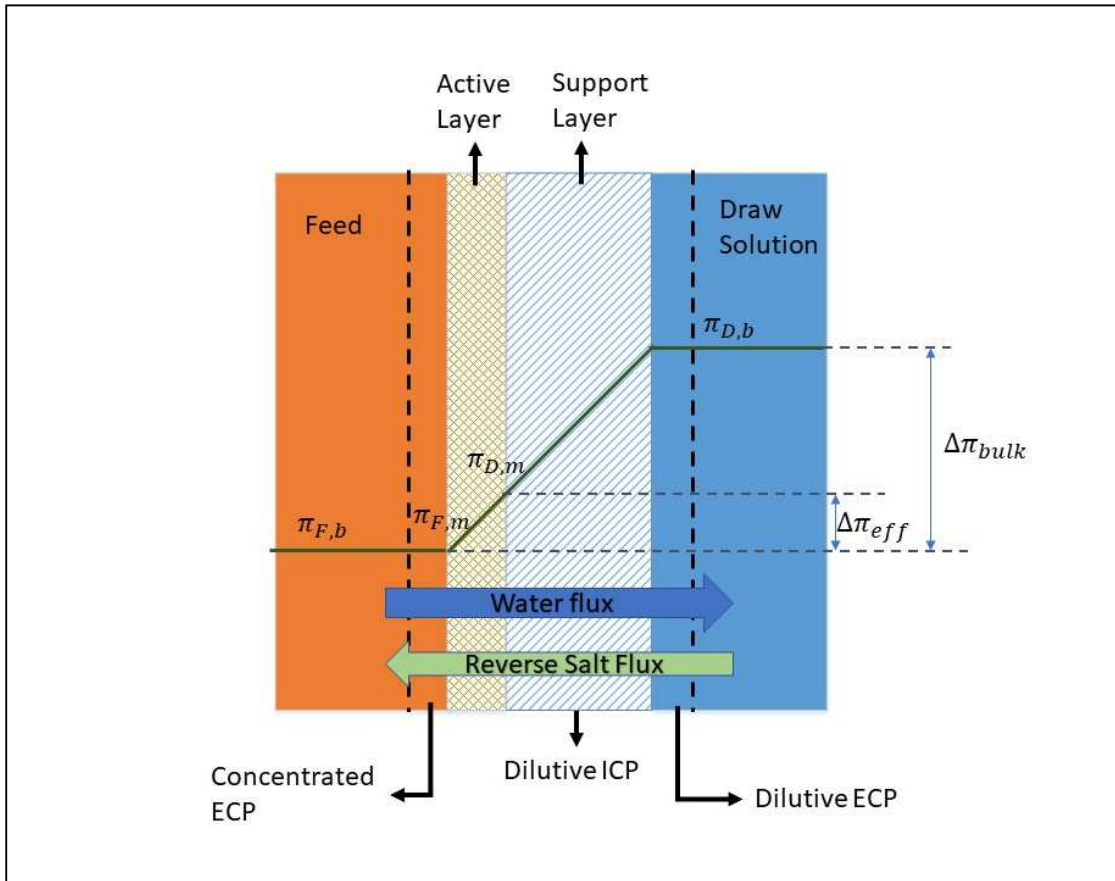
765 FO-AnMBR combines an AnMBR where the membrane is a FO membrane instead of
766 UF/MF in the conventional AnMBR process. FO relies on an osmotic gradient as a driving
767 force; and therefore, high osmotic pressure solution (seawater, seawater brine, fertilizer...)

768 also called draw solution is used to allow for permeation and extraction of water from WW
769 (feed) through the FO membrane. As such, unlike conventional AnMBR, FO-AnMBR
770 operates on the osmotic pressure difference between the feed and the draw solution with little
771 or no external hydraulic pressure. FO membranes are dense, similar to the RO membrane but
772 thinner to limit the internal concentration polarization phenomenon. Hybridization of FO-
773 AnMBR systems can be classified into various types based on membrane configuration (side-
774 stream or submerged), draw solution (DS) regeneration system (open without regeneration or
775 close with regeneration) and objective of treatment (wastewater treatment, resource recovery,
776 wastewater pre-concentration and/or reclamation).

777 FO can also be coupled with AnMBR as pre or post-treatment for concentration purposes; in
778 that case, AnMBR features a UF/MF membrane and the FO process is placed upstream or
779 downstream of AnMBR. Pre-concentration of domestic wastewater may allow for higher
780 COD load in the AnMBR and therefore optimized operation (Bao et al., 2019; Ferrari et al.,
781 2019; Wang et al., 2016; Zhang et al., 2014) and post-treatment allows the nutrient recovery
782 (Ansari et al., 2017; Xue et al., 2016) or concentration of volatile fatty acids (Blandin et al.,
783 2019).

784 Current limitations of FO were mainly low flux associated with the first generation of
785 membranes (<10LMH) and salt accumulation due to feed salt accumulation and reverse salt
786 transport from the draw solution. High cost associated with the draw solution (DS)
787 regeneration processes (Wang et al., 2016a) such as pressure-driven system (Nanofiltration or
788 Reverse osmosis) temperature-driven (membrane distillation) or electricity-driven
789 (electrodialysis) is also a point of concern (Ansari et al., 2017; Wang et al., 2016a). Water
790 flux in FO processes also reduces due to the phenomenon of concentration polarization (CP).
791 It makes the feed solution more concentrated on one side of the active layer and dilutes the
792 draw solution on the other side thus, decreasing the effective osmotic pressure driving force.

793 Based on membrane orientation i.e. active layer facing feed (AL-FS) and active layer facing
 794 draw side (AL-DS), CP has been classified into four categories i.e. concentrative and dilutive
 795 external concentration polarization (ECP) (ECP takes place on the membrane surface);
 796 concentrative and dilutive internal concentration polarization (ICP) (ICP occurs inside the
 797 support layer) (Shaffer et al., 2015). Figure 4 illustrates these phenomena.



798
 799 **Figure 4 Illustration of internal and external concentration polarization across an**
 800 **asymmetric FO membrane module. Adapted from (Gulied et al., 2020).**

801 However, recent development regarding new membranes and modules for osmotic membrane
 802 bioreactor allowing higher fluxes and very high rejection rate (including trace organic
 803 contaminants) as well as improved operation in submerged mode to limit clogging of
 804 challenging streams has opened doors to a new generation of FO-AnMBR (Blandin et al.,
 805 2018b; Blandin et al., 2016a). Salinity build-up is an inherent problem of the osmotic system
 806 and can be limited by the choice of appropriate draw solution. Finally, to limit draw recovery

807 cost, synergies can be found with other processes such as fertigation, use of waste heat (MD)
808 or combined desalination and water reuse.

809 **3.4.2. Performance comparison of FO-AnMBR with conventional AnMBR**

810 FO-AnMBR demonstrated higher removal efficiencies (96% organics, 100% total phosphate
811 and about 62% ammonia nitrogen removal) than conventional AnMBR due to the use of
812 dense FO membranes (Chen et al., 2014). FO-AnMBR has also shown a higher methane
813 yield i.e. 0.25-0.3 L CH₄/g COD (treating dilute wastewater under mesophilic conditions)
814 than conventional AnMBR (0.21 L CH₄/g COD at 25°C). It was reported that FO-AnMBR
815 has lower fouling propensity than conventional MBRs due to the absence of hydraulic
816 pressure and low flux. Due to this, foulants are not pushed on the surface of the membrane
817 and hence result in less cake fouling.

818 A study by Chen et al. (2014) found out that the COD removal efficiency of FO-AnMBR was
819 higher than the conventional AnMBR. Average COD removal efficiency was 96.7% (with
820 cellulose acetate membrane) whereas in conventional AnMBR it varies from 28 to 90%.
821 Thanks to the dense FO membrane, FO-AnMBR operation also resulted in almost complete
822 phosphate removal and 60% removal of ammonia nitrogen which is favorable compared to
823 conventional AnMBR with almost no removal of ammonia nitrogen. In addition to higher
824 rejection, the longer residence time in the FO-AnMBR can lead to advanced biodegradation
825 of organics resulting in lower COD in the supernatant and permeate. For example,
826 supernatant COD was observed to be reduced from 210 mg/L to 180 mg/L as the operating
827 time proceed (Chen et al., 2014). Similar behavior was observed by (Hou et al., 2017) where
828 initially COD of the bulk increases and then after reaching a maximum value it dropped
829 down with an increase in bio-degradation rate and a decrease in flux.

830 Table 5 summarized the COD removal efficiency and methane yield of different FO-AnMBR
831 and conventional AnMBR units. Methane yield obtained was in the range of 0.21 to 0.3 L
832 CH₄ / g COD (Gu et al., 2015; Chen et al., 2014); similar to that of AnMBR (i.e. 0.23 to
833 0.27 L CH₄ / g COD at 20-35 °C in Martinez-Sosa et al., (2011)).

834 **3.4.3. Fouling and salinity build-up in FO-AnMBR**

835 Flux decline (from 9.5 to 3.5 LMH) in continuous FO-AnMBR operation was observed
836 (Chen et al., 2014) with an increase in conductivity from 1 to 20.5 mS/cm. This decline was
837 attributed to two phenomena: membrane fouling and salinity increase. Membrane fouling
838 occurred because of the attachment of foulants to the membrane surface thereby increasing
839 hydraulic resistance and reducing flux whereas retention of feed solutes (by the dense FO
840 membrane) and the reverse salt flux coming from the draw solution are the cause of the latter.
841 A similar study on osmotic MBR highlighted that salinity increase may alter bacteria
842 efficiency leading to deflocculating and enhanced fouling (Blandin et al., 2018a). Moreover,
843 the cake layer disposition on the membrane hinders the back diffusion of the salt, resulting in
844 the buildup of salt near the membrane surface. It could result in cake-enhanced osmotic
845 pressure and lead to a reduction in the net driving force.

846 The presence of both protein and polysaccharides contributes to biofouling; A review (Wang
847 et al., 2016a) commented that both EPS and SMP played a significant role. However, it was
848 observed that the biofouling in the FO membrane was mostly external and nearly fully
849 recoverable. When the membrane was rinsed and the supernatant was discharged to bring
850 conductivity back to 1 mS/cm after one cycle of operation (22 days), 94% of initial flux was
851 recovered (Chen et al., 2014).

852 **3.4.4. Fouling mitigation in FO-AnMBR**

853 Fouling mitigation can be done by modification of membrane properties, improved
854 configuration and optimization of driving force, operating parameters and control strategies
855 (Wang et al., 2016a). The effect of the driving force by using different concentrations of draw
856 solution (NaCl) on membrane flux and fouling was studied (Wang et al., 2019). With
857 increased driving force, initial flux increases but beyond a certain critical concentration the
858 flux decline rate increased drastically (0.57 LMH/day to 1.24 LMH/day when concentration
859 increased from 1 to 2 M). Moreover, an increase in the driving force resulted in more drastic
860 fouling (fouling layer thickness increases from 35.20 μm to 96.5 μm with a concentration
861 increase of 0.25 M to 2 M). Major constituents of the bio-foulant layer were found to be β -D-
862 glucopyranose, proteins and bacterial cells whose bio-volume also increased with DS
863 concentration. It is assumed that higher initial water flux increased the foulant deposition rate
864 and raised the membrane resistance thereby, aggravated the fouling resulting in severe flux
865 drop. As for MBR, evidence of critical flux has been mentioned for the osmotic system when
866 using a new generation of FO membrane (Blandin et al., 2018a; Blandin et al., 2016b) and
867 therefore similar behavior probably occurs in FO-ANMBR. Operating below critical flux
868 would lead to a more stable and sustainable operation.

869 (Hu et al., 2017) compared the impact of NaCl and MgCl_2 as draw solutions on fouling
870 behavior. Flux decline rate using MgCl_2 (0.3 LMH/day) was more severe compared to NaCl
871 (0.16 LMH/day) indicating more fouling propensity. Moreover, the fouling layer in the case
872 of MgCl_2 was 10 μm thicker than that of using NaCl as a draw solution. Enhanced fouling
873 with MgCl_2 draw solution could be caused by the bridging ability between magnesium
874 (divalent) ion and EPS. It was also observed that the fouling potential of the TFC polyamide
875 membrane was higher compared to CTA membranes since fouling was reversible up to 94%

876 of flux recovery for the CTA membrane (section 4.3) but it was not the case with TFC
877 probably as a result of higher flux.

878 **3.4.5. Salinity build-up mitigation in FO-AnMBR**

879 The salinity build-up in wastewater is a major issue to be resolved in FO-AnMBR which is
880 inherent to the FO process (dense membrane). The accumulation of salts reduces permeate
881 flux due to the loss of the osmotic gradient and can negatively impact the biological process.

882 One way to mitigate salt accumulation is to control reverse salt flux from the draw solution to
883 the FO membrane. Using divalent salts (more rejected by the FO membrane) this could be
884 envisioned. The study showed that (Tang et al., 2014) salt accumulation was greater when
885 sodium chloride was used as the draw solution (salinity = 35 mS/cm) than other salts such as
886 sodium sulfate (salinity = 11 mS/cm) under the same operating conditions in FO-AnMBR.
887 Chloride ion has a smaller size than sulfate, thus exhibiting higher reverse salt flux.
888 Moreover, the negatively charged FO membrane would offer more repulsion to sulfate ion
889 than chloride due to differences in their charge and size. However, use of sodium sulfate
890 lowered the methane production (only 2.6 % of methane in biogas compared to 12.9% as
891 NaCl was used as the draw solution). The presence of sulfate can increase the production of
892 sulfur-reducing bacteria hindering methanogens thereby affecting methane production. Thus,
893 the use of a sulfate-based draw solution needs to be considered very carefully if significant
894 methane generation is required.

895 Playing with HRT and SRT (wasting sludge to discharge accumulated salts) is an alternative
896 to mitigate salt accumulation but should be controlled carefully and reduced SRT may
897 negatively impact the process economics (Wang et al., 2016a). Another way to mitigate
898 salinity build-up during the operating cycle is to couple a MF membrane with FO-AnMBR
899 (Wang et al., 2017). Cellulose triacetate (CTA) FO membrane and polyvinylidene fluoride

900 (PVDF) MF membrane was submerged together into an anaerobic bioreactor with 0.5M NaCl
901 of draw solution at 25 °C and at a biogas sparging rate of 2 L/min. It was found that the
902 conductivity of the mixed liquor remained stable and low (2.5 – 4 mS/cm) compared to the
903 previous study using FO-AnMBR, the MF membrane acting as the salt leak. The
904 performances of both MF and FO membranes were in accordance with conventional AnMBR
905 and FO-AnMBR yielding 90% and 96% of TOC removal efficiency, respectively. Also,
906 methane yield ranged from 0.25 to 0.28 L CH₄/g COD. However, the fouling on the FO
907 membrane was severe compared to conventional FO membranes because the permeate flux
908 could not be recovered after chemical cleaning at the end of the operation (101 days).

909 **3.5. Microbial Electrolysis Cell-AnMBR**

910 Applying an electrical field in an anaerobic membrane process by coupling MEC and
911 AnMBR is an innovative way to reduce membrane fouling (Ding et al., 2018). A PVDF
912 hollow fiber membrane was submerged into a MEC where titanium mesh and carbon were
913 used as cathode and anode respectively at external circuit resistance of 10 Ω and 36 hours of
914 HRT. Voltage ranging from 0 to 1.2 V was employed to study the removal efficiency and
915 fouling behavior of the system. COD removal with the voltage applied was about 20 %
916 higher than that without it. However, COD removal was not constant with time but decreased
917 slowly indicating a negative effect of high voltage on degradation kinetics of organic
918 contaminants. This degradation was due to increased plasmatorrhesis, reduced metabolic
919 activity and decrease in microorganism growth rate. Hence, there is a need to optimize
920 voltage for maximum efficiency.

921 The rapid decline in resistance from 400 Ω at 0.4 V to 66.67 Ω at 0.6 V indicates the potential
922 for fouling mitigation. Moreover, with an increase in applied voltage, cycle length, defined as
923 the time of operation before cleaning is required, increased (60 h at 0.4 V to 98 h at 1 V)
924 showing a reduction in cleaning requirement and hence lower fouling. The increasing voltage

925 from 0 V to 1 V in MEC-AnMBR increases the zeta-potential from 22.3 mV to 30.9 mV.
926 Higher zeta-potential of sludge resulted in less agglomeration of it on the membrane surface
927 due to higher negative charge of the sludge, thereby reducing cake formation due to
928 increasing electrostatic repulsion between the sludge and the membrane. In addition, as per
929 DLVO theory, electrostatic repulsion will reduce the stability and compactness of the cake
930 layer thus improving permeability. A decrease in protein to carbohydrate ratio of EPS (P/C
931 ratio) was observed due to a reduction in proteins in EPS (positively charged amino acid
932 groups) resulted from lower microorganism activity and reduced substrate adsorption on
933 sludge. This will also result in increase of negative charge of the cake as less amino groups
934 will be present to neutralize the negative charge of carboxyl groups and phosphoric acid
935 groups and thus making it less sticky. A decrease in sludge viscosity from 4.3 mPa.s to 3.3
936 mPa.s at 0 V and 1V, respectively was observed and the sludge adsorption capacity was
937 reduced. All these factors result in a decreasing fouling rate.

938 Another paper (Zhang et al., 2017) studied a system made by the integration of Microbial
939 Electrolysis Cell with FO-AnMBR. The MEC coupled FO-AnMBR configuration aimed at
940 providing better methane production, reducing fouling and mitigating concentration
941 polarization. The author used stainless steel mesh as a cathode which was placed in contact
942 with the membrane (cellulose triacetate based) and carbon brush as the anode. The applied
943 voltage was 0.5V. It was found that the conductivity increase rate in FO-AnMBR was 0.11
944 mS/(cm.d) whereas in MEC coupled FO-AnMBR was 0.08 mS/(cm.d) indicating less reverse
945 solute flux. The reverse flux of acetate ion was lower due to the repulsion created by the
946 negatively charged cathode and to maintain charge balance of draw solution reverse flux of
947 magnesium ion was also reduced. Application of electricity and the resultant reduction in
948 reverse solute flux decrease the salinity accumulation which indeed offers benefits like better
949 methane yield (11.07% more methane in biogas with MEC coupling compared to

950 conventional FO-AnMBR), less fouling (8.93% less loosely bound EPS and 19.3% less SMP
951 in case of MEC coupled FO-AnMBR compared to FO-AnMBR) and improved membrane
952 flux (operating cycle prolonged to 1.3 times the simple FO-AnMBR). In addition to this MEC
953 coupled FO-AnMBR provided 9.48% more COD removal efficiency compared to FO-
954 AnMBR operated under the same conditions due to degradation of the organic compound at
955 carbon anode in addition to anaerobic degradation. Moreover, the author explained that
956 protein-based EPS and SMP in the fouling layer which cause severe membrane fouling was
957 less in MEC coupled FO-AnMBR. This could be the result of electrostatic repulsion offered
958 by cathode to negatively charged protein.

959 A similar configuration but with additional recovery mode was introduced by one study (Hou
960 et al., 2017). FO-AnMBR coupled with the electrolysis system was operated at two modes,
961 initially as MEC where two carbon anodes sandwiching a Ni-based cathode were used for
962 biogas production. Later it was converted into recovery mode by placing the ionic exchange
963 membrane between the electrodes. This configuration provided benefits that include diffusion
964 of NH_4^+ through the FO membrane thus improving effluent quality, phosphorous ion
965 recovery resulting in reduced scaling, recovery of sulfate ion thus reducing methane loss due
966 to sulfate reduction and desalination of the bulk solution resulting in less osmotic pressure
967 loss.

968 During the operation, salinity build-up in MRC mode was less (0.7 to 12.7 mS/cm in 11 days)
969 compared to MEC mode (0.7 to 17 mS/cm in 11 days). This was due to ion exchange during
970 the recovery mode which was confirmed by an increase in conductivity of recovery solution
971 from 1,1 to 11.25 mS/cm. Corresponding to salinity build up the flux decline was observed
972 from 8.7 to 4 LMH. However, SEM analysis of the membrane indicated that bio-fouling
973 accounts for this decline rather than scaling, therefore, indicating the positive impact of MEC
974 coupling on scaling control in FO-AnMBR. The author also observed 97.3% flux recovery

975 after membrane rinsing indicating that the reversible fouling dominates. During MRC mode,
976 41 to 65% of PO₄-P was recovered from the bulk at the end of each stage, which not only
977 helped in alleviating scaling but also added to nutrient recovery.

978 Moreover, the system provided the current generation with average coulombic efficiency of
979 40% and provided a methane yield of 0.15 L CH₄/g COD. It can be concluded that the
980 coupling of MEC and FO-AnMBR systems could be advantageous not only in terms of
981 scaling mitigation and salinity control but also for nutrient and energy recovery. However,
982 further research is needed to develop technology at a larger scale and wider operating
983 conditions.

984 **3.6. Anaerobic Electrochemical Membrane Bioreactor (AnEMBR)**

985 AnEMBR combines MEC with AnMBR in such a way that the membrane act as one of the
986 electrodes and serves in both hydrogen generation and effluent filtration. This novel
987 technique uses a polymer-based hollow fiber membrane hybridized with an electrically
988 conductive material such as Ni (Sapireddy et al., 2019; Katuri et al., 2014), graphene (Werner
989 et al., 2016) or carbon nanotubes (Yang et al., 2019; Yang et al., 2018). The application of the
990 voltage in this configuration has not only improved hydrogen generation but also improves
991 the fouling reduction.

992 Yang et al., (2018) studied the fouling mechanism and performance of AnEMBR that uses
993 carbon nanotubes HF membrane as cathode and titanium mesh as the anode. It was found that
994 the application of voltage has a benefit in membrane fouling reduction. TMP in the case of
995 AnEMBR (applied voltage = -1.2V) was 35 kPa after 30 days of operation which was much
996 lower compared to the control reactor which observed 60 kPa (conventional AnMBR). It was
997 explained that these results were observed because negative potential repelled the negatively
998 charged pollutants from the membrane reducing the potential of cake formation. The electric

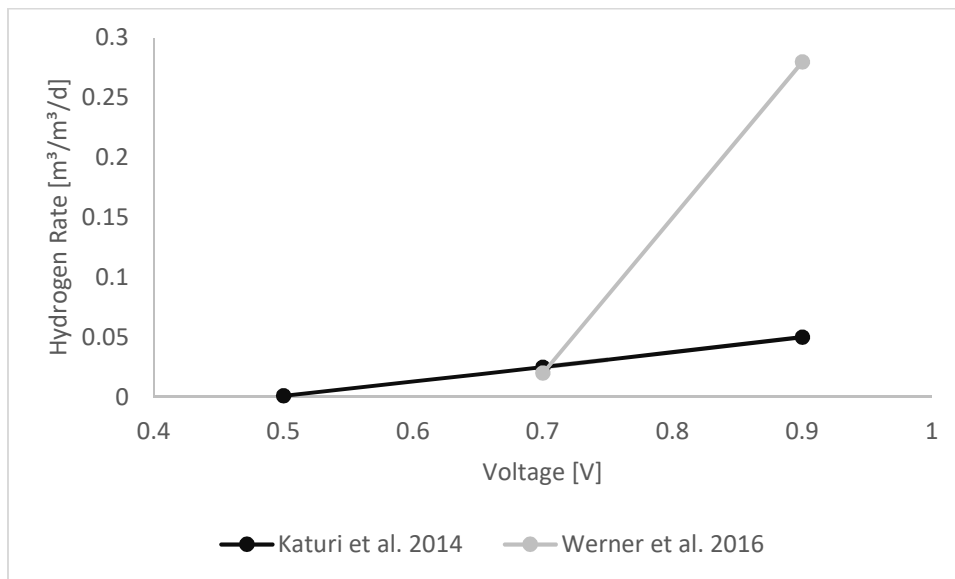
999 field also aided in the destruction of high molecular weight molecules and prevented the
1000 formation of complex cross-links between organics and divalent metal ions thus alleviating
1001 fouling. Moreover, AnEMBR showed better performance, 98% COD removal compared to
1002 95% COD removal in conventional AnMBR. Better performance can be explained by the fact
1003 that the creation of electro-active biofilm on cathode surface improved organic degradation
1004 and electric potential might have accelerated the biological degradation of organic matter.

1005 Another study (Yang et al., 2019), compared the AnEMBR with and without voltage
1006 application with a conventional AnMBR and found out similar results for COD removal and
1007 TMP i.e. in the case of electro-assisted AnEMBR (-1.2 V applied voltage). COD removal was
1008 higher than 95% and TMP was 35 kPa, whereas for AnEMBR and AnMBR COD removal
1009 was less than 95% and TMP was 50 kPa and 60 kPa, respectively. Thus, confirming that the
1010 application of voltage can not only alleviate fouling but can also improve COD removal
1011 efficiency based on the above-mentioned reasons.

1012 It further investigated the EPS content of fouled membrane to study fouling and found that
1013 protein EPS (almost 180 mg/L compared to >180 mg/L) and carbohydrates EPS (almost 150
1014 mg/L compared to >150 mg/L in AnEMBR without voltage application and >250 mg/L in
1015 AnMBR) were lower in electro-assisted AnEMBR. Lower EPS prevents the formation of the
1016 gel layer, that results in severe fouling, since sticky protein EPS is limited in quantity. Lower
1017 protein EPS means lower positively charged amino acids and thus better repulsion by
1018 negative electric field thus reduction in sludge deposition. It was also observed that the
1019 application of voltage increases the CH₄ generation (an increase of more than 40 mL/g VSS d
1020 in methane yield compared to the other two reactors) by enhancing the growth of
1021 microorganism over time thus improving volatile fatty acid's degradation and improving
1022 activity of methane-producing microbes. Higher methane recovery had a very positive effect

1023 on the overall energy balance of the system and maximum surplus energy of 51.46 kJ/day
1024 was calculated in the system.

1025 Other studies (Werner et al., 2016; Katuri et al., 2014) also found that increase in applied
1026 voltage in AnEMBR systems help in fouling mitigation. At higher voltage, hydrogen
1027 production is increased (Figure 5) which acts as an additional scouring agent and reduces
1028 fouling. Increased hydrogen production was because at higher voltage COD removal was
1029 faster (due to high current density) hence cycle time was slower, so hydrogen was dominant
1030 because the rate of hydrogen production was higher than the rate of hydrogen consumption
1031 by methanogenic bacteria.



1032
1033 ***Figure 5 Hydrogen Rate at Different Applied Voltage***

1034 One research (Sapireddy et al., 2019) demonstrates the effect of cathode surface area by
1035 operating three AnEMBR, for acetate removal, with Ni-based Hollow fiber membrane as the
1036 cathode, of specific cathode surface area (SCSA) of 2 m²/m³, 4 m²/m³ and 8 m²/m³
1037 respectively. The applied voltage was 0.7 V and the flux of 16 LMH. Acetate removal was
1038 almost similar in the case of all three AnEMBR and range between 77 to 94% throughout the
1039 operation. Coulombic efficiency is higher at the beginning of operation when hydrogen is
1040 dominant (cathode recovery of hydrogen being 77.00 ± 3.05% and that of methane being 0.82

1041 $\pm 0.26\%$ in case of SCSA of $8 \text{ m}^2/\text{m}^3$) in gas and decreases as methane generation (cathode
1042 recovery of hydrogen being $24 \pm 2.29 \%$ and that of methane being $16.9 \pm 1.02 \%$ in case of
1043 SCSA of $8 \text{ m}^2/\text{m}^3$) increases. Hydrogen being an electron donor account for this behavior.

1044 In terms of biofouling AnEMBR with SCSA of $8 \text{ m}^2/\text{m}^3$ showed the best performance with
1045 the lowest TMP. Higher hydrogen flux and increased bubble frequency with more proportion
1046 of small-sized bubbles are responsible for this behavior. Hydrogen was found to be more
1047 efficient in TMP control because of its faster evolution (less time required for molecular
1048 diffusion), higher gas velocity due to less density ($0.0898 \text{ kg}/\text{m}^3$) than methane ($0.656 \text{ kg}/\text{m}^3$)
1049 and higher gas volume since one mole of acetate produces 4 moles of hydrogen and one mole
1050 of methane. Higher bubble frequency produced more scouring effect due to increased bubble
1051 velocity and thus result in lower TMP. Moreover, smaller the size of the bubble better will be
1052 the scouring since small bubbles have higher slip velocity (velocity of gas relative to liquid)
1053 and shear force.

1054 **3.7. Vibration application in AnMBR**

1055 Vibratory shear enhancement process (VSEP) was first commercially introduced in flat sheet
1056 membranes by Armando and Culkin (New Logic International Inc, 1992). Shear forces
1057 generated by vibrations result in increased turbulence which enhances the removal of cake as
1058 the forces that were induced by shear dominated the physicochemical interactions between
1059 membrane and foulants and reduce cake layer fouling. Vibrations have a limited effect on the
1060 small foulants that can adsorb inside pores and cause pore blocking. However, since in
1061 AnMBR treating domestic wastewater cake layer fouling phenomenon dominates (Chen et
1062 al., 2014) use of vibrations can serve as a good mitigation technique. There are two ways of
1063 vibrations generation; shaker generated oscillations in liquid with a stationary membrane
1064 and/or vibrating or rotating membrane on a rotor where the liquid is held stationary (Kola et
1065 al., 2014). One study (Kola et al., 2014) demonstrated the effectiveness of transverse

1066 membrane rotation in HF AnMBR with increasing MLSS. At increased MLSS, conventional
1067 methods of fouling mitigation like gas sparging are not effective because increased viscosity
1068 greatly reduces the velocity of rising bubbles and thus reduces shear force. It was observed
1069 that at a vibration frequency of 6.7 Hz, a constant flux of 26 LMH could be maintained with
1070 increase in MLSS from 0.005 g/L to 5 g/L which in the absence of vibration decreased from
1071 16 LMH (0.005 g/L MLSS) to 1 LMH (5 g/L MLSS). This indicated that vibrations produce
1072 enough shear to counter fouling even with increasing MLSS. Increasing the frequency of
1073 vibrations from 6.7 Hz to 20 Hz effects the hydrodynamic conditions in the reactor resulting
1074 in more turbulence (Reynolds number increases from 365 to 1095 respectively) which creates
1075 the higher shear rate i.e. (1372 1/s to 30108 1/s) thus reducing fouling and increasing critical
1076 flux from 26 LMH to 51 LMH. Additionally, when compared with gas sparging and cross
1077 velocity methods at a constant flux of 30 LMH and MLSS of 26 mg/L, the time required to
1078 reach a TMP of 60 kPa in case of vibration application was 3 times more. Similar results
1079 were observed by others (Ruigómez et al., 2016a) when they compared rotation with gas
1080 sparging and found that in case of rotation better cake redispersion was observed which
1081 improved the cycle duration by 10 times compared to gas sparging.

1082 Ruigómez et al., (2016a) observed that the fouling resistance drop from 0.16 kPa/s to 0.01
1083 kPa/s with the membrane rotation of 0 to 260 rpm respectively at a permeate flux of 14 LMH.
1084 They also found that the turbulence promotor efficiency (defined as the decrease in fouling
1085 resistance compared to initial value with mitigation technique employed) for membrane
1086 rotating at 260 rpm was 96% compared to gas sparging with specific gas demand of 3.8
1087 $\text{m}^3/(\text{m}^2.\text{h})$ which has the turbulence promotor efficiency of 44.4% at a flux of 8 LMH in both
1088 the cases. This difference was observed because, in the case of membrane rotation, vibration
1089 energy is more uniformly distributed compared to sparging thus provides better shear.
1090 Another study (Mertens et al., 2019) also found improved fouling mitigation (10 times less

1091 fouling resistance at a flux of 20 LMH) by increasing shear rate from 0 s^{-1} to 605 s^{-1} in their
1092 magnetically induced membrane vibration (MMV) AnMBR system. They also found out that
1093 with a system of 4 modules, the contribution of the MMV system to total energy was only
1094 12% of total consumption.

1095 It was found that by increasing vibration from 0 Hz to 13.3 Hz, the critical flux increase by
1096 3.7 times. However, the critical flux at 20 Hz was only 24 % of that at 13.3 Hz (Kola et al.,
1097 2014), which is because, at higher vibrations, shear forces dominate Brownian, inertial and
1098 drag forces and thus causing particles to be moved away from the membrane surface. As a
1099 result of this, pore-blocking (on which vibrations have an insignificant effect) dominates. It is
1100 therefore important to select the vibration frequency carefully to optimize fouling mitigation
1101 with minimum energy demand.

1102 The effectiveness of vibrations application can be further enhanced by coupling it with
1103 periodic relaxation or backwash. For the operation of 25 days (flux = 30 LMH) when
1104 AnMBR was run at a vibrational frequency of 4.2 Hz coupled with relaxation or backwashing
1105 after 30 minutes intervals for 30 seconds (Kola et al., 2014) time required to reach a TMP of
1106 60 kPa was 100 hours for relaxation and 60 hours for backwash compared to 28 hours
1107 (approximately) with vibrations alone. The authors explained that in case of relaxation, the
1108 cake layer is loosened during relaxation and then application of vibration removed foulant
1109 thus improving the performance. In the case of backwash, when the cake layer was removed
1110 or restructured during washing (which is not the case in relaxation thus the cake layer serves
1111 as a protective layer) pore-blocking phenomenon may increase since the effectiveness of
1112 backwashing was not as high as periodic relaxation. On contrary to this, one study (Mertens
1113 et al., 2019) found backwashing to be 10 times more effective than relaxation in a 10-day
1114 operating cycle at a flux of 20 LMH and shear rate of 484 1/s where backwashing (or
1115 relaxation) time was 2 minutes after 8.5 minutes. Similarly, another study (Ruigómez et al.,

1116 2016a) conducted experiments with a filtration cycle of 12.7 minutes and cleaning duration of
1117 30 s at a rotational speed of 180 rpm and permeate flux of 8 LMH and found out that the
1118 internal fouling resistance is less in case of backwashing (11% of total) compared to that in
1119 case of relaxation (15% of total). They also coupled both backwashing and relaxation and
1120 found that optimal results were obtained at a backwashing ratio of 0.67 and a specific TMP of
1121 20 kPa. Under these conditions, reversible fouling resistance was 41% of the total and
1122 internal fouling resistance was 12% of the total. Moreover, the highest value of dispersed
1123 TSS (solid concentration of ~ 6.5 gSS/m²) was obtained under these operating conditions.

1124 From this discussion, we can conclude that the application of vibration in AnMBR operation
1125 can serve as an effective fouling mitigation technique especially if coupled with other
1126 cleaning techniques like backwashing and relaxation. However, the best-coupled combination
1127 is case dependent as it is controlled by many factors like cycle duration, permeate and
1128 backwashing flux, days of operation and cleaning time. Therefore, it is important to develop
1129 the best combination, experimentally, for employed operating conditions. To further
1130 understand the sustainability of this technique, studies must be conducted developing
1131 understanding of fouling behaviors and establishing energy balances to see the energy
1132 efficiency of vibrational systems compared to other available mitigation techniques.

1133 **3.8. Biological mitigation – Quorum Quenching**

1134 Quorum sensing (QS) is a communication technique between the cells that is used by
1135 microorganisms to control their activities like attachment or detachment, EPS formation,
1136 biofilm production and mobility. The communication is done by a generation of signal
1137 molecules that are called autoinducers e.g. N-acryl homoserine lactone (AHL). Deactivation
1138 of autoinducers results in disruption of communication between the cells and this process of
1139 deactivation is called Quorum Quenching (QQ). QQ is carried out by using QQ enzymes or

1140 bacteria that can be isolated from the sludge (Aslam et al., 2018). QQ enzymes are divided
1141 into two main types i.e. AHL-Lactonase and AHL-acylase. The former having a cleavage
1142 effect on the ester bond of the lactose ring and later breaks the amide bond. Additionally, the
1143 oxidoreductase enzyme also functions as a QQ enzyme by converting AHL to 3-hydroxy
1144 AHL thus preventing signal molecule to form bio-film (Kim et al., 2014a). Enzymatic QQ
1145 has some disadvantages such as high cost, instability and need for purification. These are
1146 overcome by the employment of QQ bacterial (Id et al., 2018). Kim et al. (2014a) have
1147 isolated 225 AHL degradation bacteria from waste sludge.

1148 Many studies in the literature have proved the effectiveness of quorum quenching in aerobic
1149 MBRs where quorum quenching bacteria has been employed in carriers like QQ beads, QQ
1150 cylinders, QQ sheets or QQ vessels (Ergön-can et al., 2017; Hyun et al., 2017; Won et al.,
1151 2016; Weerasekara et al., 2014). However, not much work has been done so far in AnMBR.
1152 The first study that has tested the effectiveness of QQ in AnMBR was published in 2019 (Liu
1153 et al., 2019) followed by two more in 2020 (Xu et al., 2020a, 2020b).

1154 Liu et al., (2019) tested four different bacterial species by entrapping them in alginate beads
1155 and then selected microbacterium sp. (a facultative anaerobe) for long term study due to its
1156 higher COD removal efficiency and higher methane production. QQ bacteria were tested in a
1157 sequence of three phases i.e. without beads (control), with empty beads (EB) and with QQ
1158 beads (QQB) respectively (Liu et al., 2019). Membrane flux was kept at 8 LMH and HRT of
1159 18.5 hours was used. COD removal efficiency during all three phases was close (97.98% for
1160 control, 98.84% for EB and 98.75% for QQB) however there is a significant difference in
1161 time required to reach TMP jump which is an indicative phenomenon for biofilm and bio-
1162 cake structural change and represent fouling in AnMBR (Zhang et al., 2006). The time
1163 requires to reach TMP in three phases was 6, 8 and 45 days, respectively. Slight improvement
1164 in the EB phase was probably due to the scouring effect. These results show the potential of

1165 QQB in fouling control in AnMBR. The effectiveness of the QQB phase was described by
1166 the analysis of AHLs concentration in the fouling layer that showed that the AHLs
1167 concentration (responsible for biofouling) in the QQB phase was lower than the control
1168 phase.

1169 Authors (Liu et al., 2019) also observed a significant reduction in EPS content (responsible
1170 for cake fouling (Chen et al., 2017a)) i.e. 15.18% reduction in the bulk phase and 75.32%
1171 reduction in the foulant layer. The protein content of EPS which is responsible for sticky cake
1172 fouling (Chen et al., 2017a) was also reduced significantly compared to the control phase
1173 (80.98% reduction). Although the QQ was found very effective in combating fouling, the
1174 AHLs degradation by single QQ species declined after 45 days. Xu et al., (2020a) proposed
1175 the use of a facultative QQ consortium and study its effect of AHLs degradation and fouling
1176 control in AnMBR.

1177 Xu et al., (2020a) studied three facultative QQ consortium consisting majorly of
1178 Proteobacteria (abundance > 90%), Firmicutes and Actinobacteria phylum isolated from
1179 activated sludge obtained from a local domestic wastewater treatment plant. All three
1180 consortiums were successful in diminishing multiple AHLs (acyl chains ranging from C4 to
1181 C10) that are responsible for biofouling in AnMBRs. The degradation rate in all cases was
1182 above 80% whereas without QQ the maximum rate obtained was 28%. It was also found that
1183 bead entrapped FQQ shows higher alleviation in EPS production (both carbohydrates and
1184 proteins) compared to free one signifying the importance of immobilization in protection
1185 against the harsh environment. FQQ with 6 carbon chain (FQQ-C6) showed the best
1186 performance in protein (72.3%) and carbohydrate (66.53%) reduction indicating its potential
1187 to mitigate fouling in AnMBR. When bead entrapped FQQ-C6 was used in AnMBR with a
1188 ceramic membrane of pore size 0.1 μm , 30 $^{\circ}\text{C}$ temperature, gas sparging rate of 0.7 L/min, 30
1189 days SRT and 17 hours HRT, a total COD removal 91% and methane yield was 0.07

1190 L/gCOD_{removed} indicating no negative effect of performance efficiency. Moreover, the
1191 presence of QQ increased the average operating period of filtration cycles by 75%, indicating
1192 efficient fouling mitigation. All these results showed the potential of QQ for fouling
1193 mitigation in AnMBR however, extensive research is required to understand the potential of
1194 long-term operation and scale-up.

1195 **4. Future perspective**

1196 AnMBR technologies allow positive energy treatment of domestic wastewater with
1197 optimization of operating conditions and fouling control strategies. Innovative mitigation
1198 techniques and process configurations are trying to resolve the issues of fouling that account
1199 for the biggest chunk of energy demand. Recent literature on lab-scale studies has suggested
1200 interesting and innovative solutions. Hybrid Processes like G-AnMBR, cell entrapment
1201 AnMBR, FO-AnMBR, MEC-AnMBR and dynamic AnMBR have shown lower fouling rate
1202 and higher % COD removal and methane yield than conventional AnMBR (Table 6).
1203 However, these are in very early stages of development and for scale-up, there is a need for
1204 an extensive study of the fouling mechanism, change in this mechanism with changing
1205 conditions and energy balance of the whole process. It is also important that the results of
1206 lab-scale studies should be validated at a larger scale and long-term studies should be
1207 conducted to broaden the range of practical application.

1208 The application of QQ in AnMBR showed promising results (Table 6) both in terms of
1209 energy-saving and production, fouling control and % COD removal. It will be interesting to
1210 apply QQ in other configurations e.g. FO-AnMBR, AnDMBR, etc. and evaluate technical
1211 and economic feasibility. Another fascinating approach can be the coupling of the electric
1212 field or vibrations with QQ and study their effect on fouling control. However, these
1213 technologies require extensive research to understand and express their full potential.

1214 Moreover, methane loss, especially under psychrophilic conditions (10-30 °C) is an area that
1215 requires more research covering the maximization of methane yield and minimization of
1216 methane leaks in the dissolved phase. Integration of methane recovery units (like membrane
1217 degassing units), improvement of membrane materials and reduction of operating energy
1218 should be given attention.

1219 Other research areas that can positively contribute towards fouling mitigation in AnMBRs
1220 and help in making them water resource recovery facilities may include,

- 1221 • Improved membrane materials with anti-fouling capabilities;
- 1222 • Coupling of different hybrid processes to combine benefits and minimize
1223 disadvantages, for example, the coupling of MEC with FO-AnMBR or Vibrations
1224 with different hybrid AnMBRs;
- 1225 • Post-treatment step integration with AnMBR for nutrient recovery. They may include
1226 adsorption, ion exchange, microalgae cultivation and forward or reverse osmosis
1227 (Shahid et al., 2020);
- 1228 • Studies involving complete plant energy assessment to analyze the effect of the
1229 secondary operation, e.g. DS re-concentration in FO-AnMBR, methane recovery unit
1230 for psychrophilic AnMBRs, entrapment procedures and sludge modification
1231 techniques, on net power generation of the process;
- 1232 • Life cycle assessment and cost-benefit studies of processes to evaluate the
1233 environmental impacts and implications.

1234 **5. Conclusion**

1235 Membrane fouling is a serious concern in the treatment of domestic wastewater treatment
1236 using AnMBR. At the pilot-scale, biogas sparging is the most employed fouling mitigation
1237 strategy but it accounts for a huge percentage of total energy requirements. Membrane

1238 material, membrane module, reactor configuration, operating conditions and sludge
1239 properties contribute towards fouling behavior as well as net energy requirements of
1240 AnMBR. Some hybrid processes have been proved to successfully reduce fouling problems
1241 of AnMBR and could be more suitable for efficient resource recovery. Additionally,
1242 applications of the electric field, voltage and vibrations have contributed positively towards
1243 fouling control. However, increasing their value beyond a certain limit will not only reduce
1244 performance efficiency but also unnecessarily increase the energy demand. Biological
1245 techniques like quorum quenching are found to be equally successful in fouling mitigation in
1246 AnMBR as they were in AeMBR and have good potential in this area especially if coupled
1247 with other techniques of fouling mitigation.

1248 **Acknowledgments**

1249 This work was supported by a grant overseen by the French National Research Agency
1250 (ANR) as part of the “JCJC” Program BàMAn (ANR-18-CE04-0001-01) and by the National
1251 Research Foundation of Korea (NRF) grant funded by the Korea government (MIST)
1252 (2019R1A2C1087530) and by TECNIO spring research grant from the People Programme
1253 (Marie Curie Actions) of the Seventh Framework Programme of the European Union
1254 (FP7/2007-2013) under REA grant agreement no. 600388 and from the Agency for Business
1255 Competitiveness of the Government of Catalonia, ACCIÓ.

1256 The author also thanks to the European Commission - Education, Audiovisual and Culture
1257 Executive Agency (EACEA) for the Erasmus Mundus scholarship under the program:
1258 Erasmus Mundus Master in Membrane Engineering for a Sustainable World (EM3E-4SW),
1259 Project Number: 574441-EPP-1-2016-1-FR-EPPKA1-JMD-MOB

Table 1. Description of different AnMBR configurations for domestic wastewater treatment (GSP: Gas Sparging, PSP: Particle Sparging, FS: Flat sheet, HF: Hollow Fiber, UF: Ultrafiltration, MF: Microfiltration, RMEM: Rotating membrane).

N°	Configuration	Membrane Module	Material	COD (% removal)	Organic Loading Rate (kg _{COD} /(m ³ .d))	References
Config-1	GSP-FS	FS UF	(PES)	>90	0.6 - 1.1	(Martinez-Sosa et al., 2011)
Config-2	GSP-HF1	HF UF	PURON (Polyester)	87	1.03-2.11	(Giménez et al., 2014)
Config-3	GSP-HF2	HF UF	PURON (Polyester)	85	0.3-1.1	(Robles et al., 2012)
Config-4	GSP-HF3	HF UF	PURON (Polyester)	85	1.25-2.24	(Robles et al., 2013)
Config-5	GSP-HF4	HF UF	PURON (Polyester)	>90	0.25-1.24	(Giménez et al., 2014)
Config-6	GSP-HF5	HF MF	RF-1 (PVDF)	87	3	(Mei et al., 2017)
Config-7	GSP-HF6	HF UF	ZeeWeed 500 (PVDF)	93.7	1.1	(Dong et al., 2015; Shin & Bae, 2018)
Config-8	GSP-HF7	HF UF	ZW-10 Zenon (PVDF)	87	1.2 - 1.44	(Gouveia et al., 2015a)
Config-9	GSP-HF8	HF UF	ZW-10 Zenon (PVDF)	90	1.6 - 2.0	(Gouveia et al., 2015b)
Config-10	GSP-HF9	HF UF	GE ZeeWeed 500 (PVDF)	93	3.77-4.97	(Dong et al., 2016)
Config-11	GSP-HF10	HF UF	W-10 Zenon, GE (PVDF)	>90	0.8-1.8	(Evans et al., 2019)
Config-12	PSP-HF	HF UF	Cheil Industries (PVDF)	>90	NA	(Shin et al., 2014)
Config-13	RMEM-HF	HF UF	GE Water & Process Tech (PVDF)	91	NA	(Ruigómez et al., 2016b)

Table 2. Description of different parameters in various AnMBR configurations (IG-AnMBR: Internally submerged granular AnMBR; ES-AnMBR: Externally submerged membrane bioreactor)

Configuration	Membrane Configuration	SS or VSS (g/L)	Days of Operation	GSI_m (Nm³/(m².h))	SRT (d)	HRT (h)	References
Config-1	ES-AnMBR	15-21 gSS/L	100	1.22	NA	19.2	(Martinez-Sosa et al., 2011)
Config-2	ES-AnMBR	22 gSS/L	70	0.23	70	6-20	(Giménez et al., 2011)
Config-3	ES-AnMBR	10-30 gSS/L	730	0.17-0.5	30-70	6-36	(Robles et al., 2012)
Config-4	ES-AnMBR	7-32 gSS/L	365	0.23	70	24.5-5.5	(Robles et al., 2013)
Config-5	ES-AnMBR	10-25 gSS/L	172	0.23	28.6-41.1	12.1-28.4	(Giménez et al., 2014)
Config-6	ES-AnMBR	4.7-20.1 gSS/L	340	0.31	NA	2.2	(Mei et al., 2017)
Config-7	ES-AnMBR	4 gSS/L	90	0.15	70	8.5	(Dong et al., 2015)
Config-8	ES-AnMBR	6 gVSS/L	1095	0.81–1.22	Infinite	7	(Gouveia et al., 2015a)
Config-9	ES-AnMBR	0.9-16.1 gVSS/L	1095	0.16–0.32	NA	12.8-14.2	(Gouveia et al., 2015b)
Config-10	ES-AnMBR	5-15 gSS/L	536	NA	40-70	8.5	(Dong et al., 2016)
Config-11	IG-AnMBR	4.30-7.54 gVSS/L	300	NA	60 ± 27	11 ± 3	(Evans et al., 2019)
Config-12	IG-AnMBR	0.600-1.2 gSS/L	485	NA	6.2-36	4.6-6.8	(Shin et al., 2014)
Config-13	ES-AnMBR	21.3 gSS/L	270	NA	270	33	(Ruigómez et al., 2016b)

Table 3. Water Treatment energy consumptions of different AnMBR configurations having different COD removal, critical flux and transmembrane pressure

Configuration	Fouling Control Energy (kWh/m³)	Critical Flux (LMH)	Total Energy (kWh/m³)	TMP (kPa)	References
Config-1	1.28	7	1.66	17.7	(Martinez-Sosa et al., 2011)
Config-2	0.2	10	0.26	8.0	(Giménez et al., 2014)
Config-3	0.2	12-16	0.26	40.0	(Robles et al., 2012)
Config-4	0.2	10-13.3	0.26	<10.0	(Robles et al., 2013)
Config-5	0.19	7-11	0.24	<10.0	(Giménez et al., 2014)
Config-6	0.5	6	0.64	6.0	(Mei et al., 2017)
Config-7	0.08	17	0.1	8.8	(Dong et al., 2015)
Config-8	0.19-0.5	10-14	0.25-0.65	5.0-55.0	(Gouveia et al., 2015a)
Config-9	0.04-0.1	12-14	0.05-0.13	40.0-55.0	(Gouveia et al., 2015b)
Config-10	0.09	25-27	0.11	1.5-30	(Dong et al., 2016)
Config-11	0.09-0.27	7.6-7.9	0.1-0.3	NA	(Evans et al., 2019)
Config-12	0.1	4.1-7.5	0.13	10.0-27.0	(Shin et al., 2014)
Config-13	0.23	10	0.3	1.0-2.5	(Ruigómez et al., 2016b)

Table 4. Effect of Pore Size on Flux and % COD Removal in AnDMBR

Configuration	Module	Support Material	The average Pore size of the support (μm)	Operating Flux (LMH)	% COD Removal	References
Internally Submerged	Flat Sheet	Polypropylene	10	2.2	99.5	(Ersahin et al., 2017)
Side Stream	Tubular	Nylon	61	31.25	-	(Siddiqui et al., 2018)
Internally Submerged	Flat Sheet	Nylon	75	22.5	75-90	(Hu et al., 2018b)
Internally Submerged	Hollow cylinder	Polyamide nylon	150	100	80	(Wang et al., 2018)

Table 5. Performance of Different FO-AnMBRs and AnMBRs treating domestic wastewater (FS: Flat sheet, HF: Hollow Fiber).

Configuration	Module	Temperature (°C)	Feed COD (mg/L)	Methane Yield (L CH ₄ /g COD)	COD % Removal (%)	References
Internally Submerged FO-AnMBR	FS	25	460	0.21	96.7	(Chen et al., 2014)
Internally Submerged FO-AnMBR	FS	35	460	0.25-0.3	95	(Gu et al., 2015)
Internally Submerged FO-AnMBR + MEC + MRC	FS	25	270±10	0.15	>93	(Hou et al., 2017)
Externally Submerged AnMBR	HF	33	445	0.07*	87	(Giménez et al., 2011)
Externally Submerged AnMBR	FS	35-20	630	0.27	>90	(Martinez-Sosa et al., 2011)

Table 6. Summary of Different Novel Configurations in AnMBR

Configuration	% COD Removal (%)	Fouling Rate (Pa/s)	Methane Yield (L CH ₄ /g COD)	Membrane Flux (LMH)	Organic Loading Rate (kg _{COD} /(m ³ .d))	Reference
AnMBR	90	3.33	0.27	7	0.6 - 1.1	(Martinez-Sosa et al., 2011)
G-AnMBR	92	0.005	0.16	7	-	(Chen et al., 2017b)
Entrapped Cell AnMBR	85	0.057	0.08	10.63	0.57	(Juntawang et al., 2017)
AnEMBR	98	0.014	-	23.22*	0.5	(Yang et al., 2018)
MEC-AnMBR	71	-	-	1.8**	5	(Ding et al., 2018)
FO-AnMBR	96.7	0.21	-	6.5**	0.46	(Chen et al., 2014)
Dynamic AnMBR	90	-	0.21	7	0.37	(Li et al., 2016)
AnMBR with Vibrations	-	0.11	-	26***	-	(Kola et al., 2014)
AnMBR with QQ	98.8	0.024	0.34	8	-	(Liu et al., 2019)

*Average flux provided per unit TMP

**Average value

***Critical flux at a frequency of 6.7 Hz

References

- Ahmar Siddiqui M., Dai J., Guan D., Chen G., 2018. Exploration of the formation of self-forming dynamic membrane in an upflow anaerobic sludge blanket reactor. *Sep. Purif. Technol.* 212, 757–766. <https://doi.org/10.1016/J.SEPPUR.2018.11.065>
- Alepu O.E., Segun G.A., Ikhumhen H.O., 2016. Formation mechanism and performance of dynamic membrane technology for municipal wastewater treatment - A review. *Adv. Recycl. Waste Manag.* 01, 3–8. <https://doi.org/10.4172/2475-7675.1000113>
- Alibardi L., Bernava N., Cossu R., Spagni A., 2016. Anaerobic dynamic membrane bioreactor for wastewater treatment at ambient temperature. *Chem. Eng. J.* 284, 130–138. <https://doi.org/10.1016/j.cej.2015.08.111>
- Alibardi L., Cossu R., Saleem M., Spagni A., 2014. Development and permeability of a dynamic membrane for anaerobic wastewater treatment. *Bioresour. Technol.* 161, 236–244. <https://doi.org/10.1016/j.biortech.2014.03.045>
- Amha Y.M., Corbett M., Smith A.L., 2019. Two-Phase Improves Performance of Anaerobic Membrane Bioreactor Treatment of Food Waste at High Organic Loading Rates. *Environ. Sci. Technol.* 53, 9572–9583. <https://doi.org/10.1021/acs.est.9b02639>
- Ansari A.J., Hai F.I., Price W.E., Drewes J.E., Nghiem L.D., 2017. Forward osmosis as a platform for resource recovery from municipal wastewater - A critical assessment of the literature. *J. Membr. Sci.* 529, 195–206. <https://doi.org/10.1016/j.memsci.2017.01.054>
- Aslam M., Ahmad R., Kim J., 2018. Recent developments in biofouling control in membrane bioreactors for domestic wastewater treatment. *Sep. Purif. Technol.* 206, 297–315. <https://doi.org/10.1016/j.seppur.2018.06.004>
- Aslam M., Charfi A., Lesage G., Heran M., Kim J., 2017. Membrane bioreactors for wastewater treatment: A review of mechanical cleaning by scouring agents to control membrane fouling. *Chem. Eng. J.* 307, 897–913. <https://doi.org/10.1016/j.cej.2016.08.144>
- Aslam M., McCarty P.L., Bae J., Kim J., 2014. The effect of fluidized media characteristics on membrane fouling and energy consumption in anaerobic fluidized membrane bioreactors. *Sep. Purif. Technol.* 132, 10–15. <https://doi.org/10.1016/j.seppur.2014.04.049>
- Baeten, J. E., Batstone, D. J., Schraa, O. J., van Loosdrecht, M. C., & Volcke, E. I. (2019). Modelling anaerobic, aerobic and partial nitrification-anammox granular sludge reactors- A review. *Water research*, 149, 322-341. <https://doi.org/10.1016/j.watres.2018.11.026>.
- Bao X., Wu Q., Tian J., Shi W., Wang W., Zhang Z., Zhang R., Zhang B., Guo Y., Shu S., Cui F., 2019. Fouling mechanism of forward osmosis membrane in domestic wastewater concentration: Role of substrate structures. *Chem. Eng. J.* 370, 262–273. <https://doi.org/10.1016/j.cej.2019.03.174>
- Blandin G., Gautier C., Sauchelli Toran M., Monclús H., Rodríguez-Roda I., Comas J., 2018a. Retrofitting membrane bioreactor (MBR) into osmotic membrane bioreactor (OMBR): A pilot-scale study. *Chem. Eng. J.* 339, 268–277. <https://doi.org/10.1016/j.cej.2018.01.103>

- Blandin G., Le-Clech P., Cornelissen E., Verliefde A.R.D., Comas J., Rodriguez-Roda I., 2018b. Can osmotic membrane bioreactor be a realistic solution for water reuse? *NPJ Clean Water* 1, 1–6. <https://doi.org/10.1038/s41545-018-0006-x>
- Blandin G., Rosselló B., Monsalvo V.M., Batlle-Vilanova P., Viñas J.M., Rogalla F., Comas J., 2019. Volatile fatty acids concentration in real wastewater by forward osmosis. *J. Membr. Sci.* 575, 60–70. <https://doi.org/10.1016/j.memsci.2019.01.006>
- Blandin G., Verliefde A.R.D., Comas J., Rodriguez-Roda I., Le-Clech P., 2016a. Efficiently combining water reuse and desalination through forward osmosis-reverse osmosis (FO-RO) hybrids: A critical review. *Membranes* 6, 37. <https://doi.org/10.3390/membranes6030037>
- Blandin G., Vervoort H., Le-Clech P., Verliefde A.R.D., 2016b. Fouling and cleaning of high permeability forward osmosis membranes. *J. Water Process. Eng.* 9, 161–169. <https://doi.org/10.1016/j.jwpe.2015.12.007>
- Bourgeois K.N., Darby J.L., Tchobanoglous G., 2001. Ultrafiltration of wastewater: Effects of particles, mode of operation and backwash effectiveness. *Water Res.* 35, 77–90. [https://doi.org/10.1016/S0043-1354\(00\)00225-6](https://doi.org/10.1016/S0043-1354(00)00225-6)
- Bu F., Du S., Xie L., Cao R., Zhou Q., 2017. Swine manure treatment by anaerobic membrane bioreactor with carbon, nitrogen and phosphorus recovery. *Water Sci. Technol.* 76, 1939–1949. <https://doi.org/10.2166/wst.2017.278>
- Charfi A., Amar N. Ben, Harmand J., 2012. Analysis of fouling mechanisms in anaerobic membrane bioreactors. *Water Res.* 46, 2637–2650. <https://doi.org/10.1016/j.watres.2012.02.021>
- Chen C., Guo W., Ngo H.H., 2016. Advances in granular growth anaerobic membrane bioreactor (G-AnMBR) for low strength wastewater treatment. *J. Energy Environ. Sustain.* 1, 77–83. <https://doi.org/oai:opus.lib.uts.edu.au:10453/49973>
- Chen C., Guo W., Ngo H.H., Chang S.W., Duc Nguyen D., Dan Nguyen P., Bui X.T., Wu Y., 2017b. Impact of reactor configurations on the performance of a granular anaerobic membrane bioreactor for municipal wastewater treatment. *Int. Biodeterior. Biodegrad.* 121, 131–138. <https://doi.org/10.1016/j.ibiod.2017.03.021>
- Chen C., Guo W.S., Ngo H.H., Liu Y., Du B., Wei Q., Wei D., Nguyen D.D., Chang S.W., 2017c. Evaluation of a sponge assisted-granular anaerobic membrane bioreactor (SG-AnMBR) for municipal wastewater treatment. *Renew. Energy* 111, 620–627. <https://doi.org/10.1016/j.renene.2017.04.055>
- Chen L., Gu Y., Cao C., Zhang J., Ng J.W., Tang C., 2014. Performance of a submerged anaerobic membrane bioreactor with forward osmosis membrane for low-strength wastewater treatment. *Water Res.* 50, 114–123. <https://doi.org/10.1016/j.watres.2013.12.009>
- Chen R., Nie Y., Hu Y., Miao R., Utashiro T., Li Q., Xu M., 2017a. Fouling behavior of soluble microbial products and extracellular polymeric substances in a submerged anaerobic membrane bioreactor treating low-strength wastewater at room temperature. *J. Membr. Sci.* 531, 1–9. <https://doi.org/10.1016/j.memsci.2017.02.046>
- Choo K., Lee C., 1998. Hydrodynamic behavior of anaerobic biosolids during crossflow filtration in the membrane anaerobic bioreactor. *Water Res.* 32, 3387–3397.

[https://doi.org/10.1016/S0043-1354\(98\)00103-1](https://doi.org/10.1016/S0043-1354(98)00103-1)

- Christian S., Grant S., McCarthy P., Wilson D., Mills D., 2011. The first two years of full-scale anaerobic membrane bioreactor (AnMBR) operation treating high-strength industrial wastewater. *Water Pract. Technol.* 6. <https://doi.org/10.2166/wpt.2011.032>
- Chu H., Zhang Y., Zhou X., Zhao Y., Dong B., Zhang H., 2014. Dynamic membrane bioreactor for wastewater treatment: Operation, critical flux and dynamic membrane structure. *J. Membr. Sci.* 450, 265–271. <https://doi.org/10.1016/j.memsci.2013.08.045>
- Ding A., Fan Q., Cheng R., Sun G., Zhang M., Wu D., 2018. Impacts of applied voltage on microbial electrolysis cell-anaerobic membrane bioreactor (MEC-AnMBR) and its membrane fouling mitigation mechanism. *Chem. Eng. J.* 333, 630–635. <https://doi.org/10.1016/j.cej.2017.09.190>
- Ding Y., Tian Y., Li Z., Zuo W., Zhang J., 2015. A comprehensive study into fouling properties of extracellular polymeric substance (EPS) extracted from bulk sludge and cake sludge in a mesophilic anaerobic membrane bioreactor. *Bioresour. Technol.* 192, 105–114. <https://doi.org/10.1016/j.biortech.2015.05.067>
- Dong Q., Parker W., Dagnew M., 2015. Impact of FeCl₃ dosing on AnMBR treatment of municipal wastewater. *Water Res.* 80, 281–293. <https://doi.org/10.1016/j.watres.2015.04.025>
- Dong, Q., Parker, W., & Dagnew, M. 2016. Long term performance of membranes in an anaerobic membrane bioreactor treating municipal wastewater. *Chemosphere*, 144, 249-256. <https://doi.org/10.1016/j.chemosphere.2015.08.077>
- Ergön-can T., Köse-mutlu B., Ismail İ., Lee C., 2017. Biofouling control based on bacterial quorum quenching with a new application : Rotary microbial carrier frame. *J. Membr. Sci.* 525, 116–124. <https://doi.org/10.1016/j.memsci.2016.10.036>
- Ersahin M.E., Tao Y., Ozgun H., Gimenez J.B., Spanjers H., van Lier J.B., 2017. Impact of anaerobic dynamic membrane bioreactor configuration on treatment and filterability performance. *J. Membr. Sci.* 526, 387–394. <https://doi.org/10.1016/j.memsci.2016.12.057>
- Ersahin M.E., Tao Y., Ozgun H., Spanjers H., van Lier J.B., 2016. Characteristics and role of dynamic membrane layer in anaerobic membrane bioreactors. *Biotechnol. Bioeng.* 113, 761–771. <https://doi.org/10.1002/bit.25841>
- Evans P.J., Parameswaran P., Lim K., Bae J., Shin C., Ho J., McCarty P.L., 2019. A comparative pilot-scale evaluation of gas-sparged and granular activated carbon-fluidized anaerobic membrane bioreactors for domestic wastewater treatment. *Bioresour. Technol.* 288, 120949. <https://doi.org/10.1016/j.biortech.2019.01.072>
- Ferrari F., Pijuan M., Rodriguez-Roda I., Blandin G., 2019. Exploring submerged forward osmosis for water recovery and pre-concentration of wastewater before anaerobic digestion: A pilot-scale study. *Membranes* 9, 97. <https://doi.org/10.3390/membranes9080097>
- Fulcher J., 2014. Changing the Terms | WEF News [WWW Document]. URL <https://news.wef.org/changing-the-terms/> (accessed 10.15.19).
- Galib M., Elbeshbishy E., Reid R., Hussain A., Lee H., 2016. Energy-positive food wastewater treatment using an anaerobic membrane bioreactor (AnMBR). *J. Environ.*

Manage. 182, 477–485. <https://doi.org/10.1016/j.jenvman.2016.07.098>

- Giménez J.B., Martí N., Robles A., Ferrer J., Seco A., 2014. Anaerobic treatment of urban wastewater in membrane bioreactors: Evaluation of seasonal temperature variations. *Water Sci. Technol.* 69, 1581–1588. <https://doi.org/10.2166/wst.2014.069>
- Giménez J.B., Robles A., Carretero L., Durán F., Ruano M. V., Gatti M.N., Ribes J., Ferrer J., Seco A., 2011. Experimental study of the anaerobic urban wastewater treatment in a submerged hollow-fiber membrane bioreactor at pilot-scale. *Bioresour. Technol.* 102, 8799–8806. <https://doi.org/10.1016/j.biortech.2011.07.014>
- Gouveia J., Plaza F., Garralon G., Fdz-Polanco F., Peña M., 2015a. Long-term operation of a pilot-scale anaerobic membrane bioreactor (AnMBR) for the treatment of municipal wastewater under psychrophilic conditions. *Bioresour. Technol.* 185, 225–233. <https://doi.org/10.1016/j.biortech.2015.03.002>
- Gouveia J., Plaza F., Garralon G., Fdz-Polanco F., Peña M., 2015b. A novel configuration for an anaerobic submerged membrane bioreactor (AnSMBR). Long-term treatment of municipal wastewater under psychrophilic conditions. *Bioresour. Technol.* 198, 510–519. <https://doi.org/10.1016/j.biortech.2015.09.039>
- Gu Y., Chen L., Ng J.W., Lee C., Chang V.W.C., Tang C.Y., 2015. Development of anaerobic osmotic membrane bioreactor for low-strength wastewater treatment at mesophilic condition. *J. Membr. Sci.* 490, 197–208. <https://doi.org/10.1016/j.memsci.2015.04.032>
- Gulied, M., Al Nouss, A., Khraishah, M., & AlMomani, F. (2020). Modeling and simulation of fertilizer drawn forward osmosis process using Aspen Plus-MATLAB model. *Sci. Total Environ.* 700, 134461. <https://doi.org/10.1016/j.scitotenv.2019.134461>
- Herrera-Robledo M., Cid-León D.M., Morgan-Sagastume J.M., Noyola A., 2011. Biofouling in an anaerobic membrane bioreactor treating municipal sewage. *Sep. Purif. Technol.* 81, 49–55. <https://doi.org/10.1016/j.seppur.2011.06.041>
- Holbrook R.D., Higgins M.J., Murthy S.N., Fonseca A.D., Fleischer J., Daigger G.T., Grizzard T.J., Love N.G., Novak J.T., Murthy N., Fonseca D., Grizzard J., Love N.G., Novak J.T., Fleischer J., David R., Higgins J., Daigger G.T., 2004. Effect of alum of addition on the performance of submerged membranes for wastewater treatment. *Water Environ. Res.* 76, 2699–2702. <https://doi.org/10.1002/j.1554-7531.2004.tb00232.x>
- Hou D., Lu L., Sun D., Ge Z., Huang X., Cath T.Y., Ren Z.J., 2017. Microbial electrochemical nutrient recovery in anaerobic osmotic membrane bioreactors. *Water Res.* 114, 181–188. <https://doi.org/10.1016/j.watres.2017.02.034>
- Hu A., Stuckey D., 2007. Activated carbon addition to a submerged anaerobic membrane bioreactor: Effect on performance, transmembrane pressure, and flux- *ACSE J. Environ. Eng.* 133, 73–80. [https://doi.org/10.1061/\(ASCE\)0733-9372\(2007\)133:1\(73\)](https://doi.org/10.1061/(ASCE)0733-9372(2007)133:1(73))
- Hu T., Wang X., Wang C., Li X., Ren Y., 2017. Impacts of inorganic draw solutes on the performance of thin-film composite forward osmosis membrane in a microfiltration assisted anaerobic osmotic membrane bioreactor. *RSC Adv.* 7, 16057–16063. <https://doi.org/10.1039/C7RA01524K>
- Hu Y., Wang X.C., Ngo H.H., Sun Q., Yang Y., 2018a. Anaerobic dynamic membrane bioreactor (AnDMBR) for wastewater treatment: A review. *Bioresour. Technol.* 247,

1107–1118. <https://doi.org/10.1016/j.biortech.2017.09.101>

- Hu Y., Yang Y., Yu S., Wang X.C., Tang J., 2018b. Psychrophilic anaerobic dynamic membrane bioreactor for domestic wastewater treatment: Effects of organic loading and sludge recycling. *Bioresour. Technol.* 270, 62–69. <https://doi.org/10.1016/j.biortech.2018.08.128>
- Hyun C., Choi D., Kwon H., Lee S., Hyun S., Lee K., Choo K., Lee J., Lee C., Park P., 2017. Application of quorum quenching bacteria entrapping sheets to enhance biofouling control in a membrane bioreactor with a hollow fiber module. *J. Membr. Sci.* 526, 264–271. <https://doi.org/10.1016/j.memsci.2016.12.046>
- Id A.S., Arroyo M., Mendoza A., Muras A., Cristina Á., Garc C., Marquina D., Santos A., Serrano S., 2018. Quorum sensing versus quenching bacterial isolates obtained from MBR plants treating leachates from municipal solid waste. *Int. J. Env. Res. Pub. HE.* 15, 1019. <https://doi.org/10.3390/ijerph15051019>
- Jain M., 2018. Anaerobic membrane bioreactor as highly efficient and reliable technology for wastewater treatment — A review. *Adv. Chem. Engineer. Sci.* 08, 82–100. <https://doi.org/10.4236/aces.2018.82006>
- Jeison D., Betuw W. Van, Lier J.B. Van, 2008. Feasibility of anaerobic membrane bioreactors for the treatment of wastewaters with particulate organic matter feasibility of anaerobic membrane bioreactors. *Sep. Sci. Technol.* 43, 3417–3431. <https://doi.org/10.1080/01496390802221659>
- Jiang T., Zhang H., Gao D., Dong F., Gao J., Yang F., 2012. Fouling characteristics of a novel rotating tubular membrane bioreactor. *Chem. Eng. Process.* 62, 39–46. <https://doi.org/10.1016/j.cep.2012.09.012>
- Judd S., 2011. *The MBR book: principles and applications of membrane bioreactors for water and wastewater treatment.*, 2nd ed. Elsevier.
- Judd S., Broeke L.J.P. Van Den, Shurair M., Kuti Y., Znad H., 2015. Algal remediation of CO₂ and nutrient discharge: A review. *Water Res.* 87, 356–366. <https://doi.org/10.1016/j.watres.2015.08.021>
- Juntawang C., Rongsayamanont C., Khan E., 2019. Entrapped-cells-based anaerobic forward osmosis membrane bioreactor treating medium-strength domestic wastewater: Fouling characterization and performance evaluation. *Chemosphere* 225, 226–237. <https://doi.org/10.1016/j.chemosphere.2019.03.032>
- Juntawang C., Rongsayamanont C., Khan E., 2017. Entrapped cells-based-anaerobic membrane bioreactor treating domestic wastewater: Performances, fouling, and bacterial community structure. *Chemosphere* 187, 147–155. <https://doi.org/10.1016/j.chemosphere.2017.08.113>
- Kanai, M., Ferre, V., Wakahara, S., Yamamoto, T., Moro, M., 2010. A novel combination of methane fermentation and MBR - Kubota Submerged Anaerobic Membrane Bioreactor process. *Desalination* 250, 964–967. <https://doi.org/10.1016/j.desal.2009.09.082>
- Katuri K.P., Werner C.M., Jimenez-sandoval R.J., Chen W., Jeon S., Logan B.E., Lai Z., Amy G.L., Saikaly P.E., 2014. A novel anaerobic electrochemical membrane bioreactor (AnEMBR) with conductive hollow- fiber membrane for treatment of low- organic strength solutions. *Environ. Sci. Technol.* 48, 12833–12841.

<https://doi.org/10.1021/es504392n>

- Kim A., Park S., Lee Chi-ho, Lee Chung-hak, Lee J., 2014a. Quorum quenching bacteria isolated from the sludge of a wastewater treatment plant and their application for controlling biofilm formation. *J. Microbiol. Biotechn.* 24, 1574–1582. <https://doi.org/10.4014/jmb.1407.07009>
- Kim J., Kim K., Ye H., Lee E., 2011. Anaerobic fluidized bed membrane bioreactor for wastewater treatment. *Environ. Sci. Technol.* 45, 576–581. <https://doi.org/10.1021/es1027103>
- Kim J., Shin J., Kim H., Lee J.Y., Yoon M. hyuk, Won S., Lee B.C., Song K.G., 2014. Membrane fouling control using a rotary disk in a submerged anaerobic membrane sponge bioreactor. *Bioresour. Technol.* 172, 321–327. <https://doi.org/10.1016/j.biortech.2014.09.013>
- Kola A., Ye Y., Le-Clech P., Chen V., 2014. Transverse vibration as novel membrane fouling mitigation strategy in anaerobic membrane bioreactor applications. *J. Membr. Sci.* 455, 320–329. <https://doi.org/10.1016/j.memsci.2013.12.078>
- Krzeminski P., Graaf J.H., J. M. van der, Lier J.B.. van, 2012. Specific energy consumption of membrane bioreactor (MBR) for sewage treatment. *Water Sci. Technol.* 65, 380–392. <https://doi.org/10.2166/wst.2012.861>
- Krzeminski P., Leverette L., Malamis S., Katsou E., 2017. Membrane bioreactors – A review on recent developments in energy reduction, fouling control, novel configurations, LCA and market prospects. *J. Membr. Sci.* 527, 207–227. <https://doi.org/10.1016/j.memsci.2016.12.010>
- Laspidou C.S., Rittmann B.E., 2002. A unified theory for extracellular polymeric substances, soluble microbial products, and active and inert biomass. *Water Res.* 36, 2711–2720. [https://doi.org/10.1016/S0043-1354\(01\)00413-4](https://doi.org/10.1016/S0043-1354(01)00413-4)
- Li N., He L., Lu Y.Z., Zeng R.J., Sheng G.P., 2017. Robust performance of a novel anaerobic biofilm membrane bioreactor with mesh filter and carbon fiber (ABMBR) for low to high strength wastewater treatment. *Chem. Eng. J.* 313, 56–64. <https://doi.org/10.1016/j.cej.2016.12.073>
- Li N., Hu Y., Lu Y.Z., Zeng R.J., Sheng G.P., 2016. In-situ biogas sparging enhances the performance of an anaerobic membrane bioreactor (AnMBR) with mesh filter in low-strength wastewater treatment. *Appl. Microbiol. Biot.* 100, 6081–6089. <https://doi.org/10.1007/s00253-016-7455-2>
- Lin H., Chen J., Wang F., Ding L., Hong H., 2011. Feasibility evaluation of submerged anaerobic membrane bioreactor for municipal secondary wastewater treatment. *Desalination* 280, 120–126. <https://doi.org/10.1016/j.desal.2011.06.058>
- Lin H., Peng W., Zhang M., Chen J., Hong H., Zhang Y., 2013. A review on anaerobic membrane bioreactors: Applications, membrane fouling and future perspectives. *Desalination* 314, 169–188. <https://doi.org/10.1016/j.desal.2013.01.019>
- Liu J., Yee C., Shin J., Haur T., Wang L., 2019. Quorum quenching in anaerobic membrane bioreactor for fouling control. *Water Res.* 156, 159–167. <https://doi.org/10.1016/j.watres.2019.03.029>
- Martin-Garcia I., Monsalvo V., Pidou M., Le-Clech P., Judd S.J., McAdam E.J., Jefferson B.,

2011. Impact of membrane configuration on fouling in anaerobic membrane bioreactors. *J. Membr. Sci.* 382, 41–49. <https://doi.org/10.1016/j.memsci.2011.07.042>
- Martin I., Pidou M., Soares A., Judd S., Jefferson B., 2011. Modeling the energy demands of aerobic and anaerobic membrane bioreactors for wastewater treatment. *Environ. Technol.* 32, 921–932. <https://doi.org/10.1080/09593330.2011.565806>
- Martinez-Sosa D., Helmreich B., Netter T., Paris S., Bischof F., Horn H., 2011. Anaerobic submerged membrane bioreactor (AnSMBR) for municipal wastewater treatment under mesophilic and psychrophilic temperature conditions. *Bioresour. Technol.* 102, 10377–10385. <https://doi.org/10.1016/j.biortech.2011.09.012>
- McCarty P.L., Bae J., Kim J., 2011. Domestic wastewater treatment as a net energy producer—can this be achieved? *Environ. Sci. Technol.* 45, 7100–7106. <https://doi.org/10.1021/es2014264>
- Mei X., Wang Z., Miao Y., Wu Z., 2017. A pilot-scale anaerobic membrane bioreactor under short hydraulic retention time for municipal wastewater treatment: performance and microbial community identification. *J. Water. Reuse. Desal.* 8, 58–67. <https://doi.org/10.2166/wrd.2017.164>
- Mertens M., Quintelier M., Vankelecom I.F.J., 2019. Magnetically induced membrane vibration (MMV) system for wastewater treatment. *Sep. Purif. Technol.* 211, 909–916. <https://doi.org/10.1016/j.seppur.2018.08.060>
- New Logic International Inc, 1992. New separation system extends the use of membranes in Filtration and Separation. Elsevier, pp. 376–378. [https://doi.org/10.1016/0015-1882\(92\)80196-P](https://doi.org/10.1016/0015-1882(92)80196-P)
- Pretel R., Robles A., Ruano M. V., Seco A., Ferrer J., 2016. A plant-wide energy model for wastewater treatment plants: Application to anaerobic membrane bioreactor technology. *Environ. Technol.* 37, 2298–2315. <https://doi.org/10.1080/09593330.2016.1148903>
- Pretel R., Robles A., Ruano M. V., Seco A., Ferrer J., 2014. The operating cost of an anaerobic membrane bioreactor (AnMBR) treating sulphate-rich urban wastewater. *Sep. Purif. Technol.* 126, 30–38. <https://doi.org/10.1016/j.seppur.2014.02.013>
- Quek P.J., Yeap T.S., Ng H.Y., 2017. Applicability of upflow anaerobic sludge blanket and dynamic membrane-coupled process for the treatment of municipal wastewater. *Applied Microbiology and Biotechnology* 101, 6531–6540. <https://doi.org/10.1007/s00253-017-8358-6>
- Robles A., Ruano M. V., Ribes J., Ferrer J., 2013. Performance of industrial-scale hollow-fiber membranes in a submerged anaerobic MBR (HF-SAnMBR) system at mesophilic and psychrophilic conditions. *Sep. Purif. Technol.* 104, 290–296. <https://doi.org/10.1016/j.seppur.2012.12.004>
- Robles A., Ruano M. V., García-usach F., Ferrer J., 2012. Sub-critical filtration conditions of commercial hollow-fiber membranes in a submerged anaerobic MBR (HF-SAnMBR) system: The effect of gas sparging intensity. *Bioresour. Technol.* 114, 247–254. <https://doi.org/10.1016/j.biortech.2012.03.085>
- Robles Á., Victoria M., Char A., Heran M., Harmand J., Seco A., Steyer J., Batstone D.J., Kim J., 2018. A review on anaerobic membrane bioreactors (AnMBRs) focused on modeling and control aspects. *Bioresour. Technol.* 270, 612–626.

<https://doi.org/10.1016/j.biortech.2018.09.049>

- Ruigómez I., González E., Guerra S., Rodríguez-gómez L.E., Vera L., 2017. Evaluation of a novel physical cleaning strategy based on HF membrane rotation during the backwashing/relaxation phases for anaerobic submerged MBR. *J. Membr. Sci.* 526, 181–190. <https://doi.org/10.1016/j.memsci.2016.12.042>
- Ruigómez I., Vera L., González E., González G., Rodríguez-sevilla J., 2016a. A novel rotating HF membrane to control fouling on anaerobic membrane bioreactors treating wastewater. *J. Membr. Sci.* 501, 45–52. <https://doi.org/10.1016/j.memsci.2015.12.011>
- Ruigómez I., Vera L., González E., Rodríguez-Sevilla J., 2016b. Pilot plant study of a new rotating hollow fibre membrane module for improved performance of an anaerobic submerged MBR. *J. Membr. Sci.* 514, 105–113. <https://doi.org/10.1016/j.memsci.2016.04.061>
- Saleem M., Alibardi L., Lavagnolo M.C., Cossu R., Spagni A., 2016. Effect of filtration flux on the development and operation of a dynamic membrane for anaerobic wastewater treatment. *J. Environ. Manage.* 180, 459–465. <https://doi.org/10.1016/j.jenvman.2016.05.054>
- Sapireddy V., Katuri K.P., Yu Y., Lai Z., Li E., Thoroddsen S.T., Saikaly P.E., 2019. Effect of specific cathode surface area on biofouling in an anaerobic electrochemical membrane bioreactor: Novel insights using high-speed video camera. *J. Membr. Sci.* 577, 176–183. <https://doi.org/10.1016/j.memsci.2019.02.007>
- Shaffer, D. L., Werber, J. R., Jaramillo, H., Lin, S., & Elimelech, M. (2015). Forward osmosis: Where are we now? *Desalination*, 356, 271–284. <https://doi.org/10.1016/j.desal.2014.10.031>
- Shahid, M.K., Kashif, A., Rout, P.R., Aslam, M., Fuwad, A., Choi, Y., Banu J, R., Park, J.H., Kumar, G., 2020. A brief review of anaerobic membrane bioreactors emphasizing recent advancements, fouling issues and future perspectives. *J. Environ. Manage.* 270, 110909. <https://doi.org/10.1016/j.jenvman.2020.110909>
- Shin C., Bae J., 2018. Current status of the pilot-scale anaerobic membrane bioreactor treatments of domestic wastewaters: A critical review. *Bioresour. Technol.* 247, 1038–1046. <https://doi.org/10.1016/j.biortech.2017.09.002>
- Shin C., McCarty P.L., Kim J., Bae J., 2014. Pilot-scale temperate-climate treatment of domestic wastewater with a staged anaerobic fluidized membrane bioreactor (SAF-MBR). *Bioresour. Technol.* 159, 95–103. <https://doi.org/10.1016/j.biortech.2014.02.060>
- Shoener B.D., Cheng Z., Greiner A.D., Khunjar W., Hong P.-Y., Guest J.S., 2016. Design of anaerobic membrane bioreactors for the valorization of dilute organic carbon waste streams. *Energy Environ. Sci.* 9, 1102–1112. <https://doi.org/10.1039/C5EE03715H>
- Skouteris G., Hermosilla D., López P., Negro C., Blanco Á., 2012. Anaerobic membrane bioreactors for wastewater treatment: A review. *Chem. Eng. J.* 198–199, 138–148. <https://doi.org/10.1016/j.cej.2012.05.070>
- Smith A.L., Stadler L.B., Cao L., Love N.G., Raskin L., Skerlos S.J., 2014. Navigating wastewater energy recovery strategies: A life cycle comparison of anaerobic membrane bioreactor and conventional treatment systems with anaerobic digestion. *Environ. Sci. Technol.* 48, 5972–81. <https://doi.org/10.1021/es5006169>

- Smith A.L., Stadler L.B., Love N.G., Skerlos S.J., Raskin L., 2012. Perspectives on anaerobic membrane bioreactor treatment of domestic wastewater: A critical review. *Bioresour. Technol.* 122, 149–159. <https://doi.org/10.1016/j.biortech.2012.04.055>
- Sun F., Zhang N., Li F., Wang X., Zhang J., Song L., Liang S., 2018. Dynamic analysis of self-forming dynamic membrane (SFDM) filtration in submerged anaerobic bioreactor: Performance, characteristic, and mechanism. *Bioresour. Technol.* 270, 383–390. <https://doi.org/10.1016/j.biortech.2018.09.003>
- Taghipour S, Ayati B, Razaei M. Study of the SBAR performance in COD removal of Petroleum and MTBE. *IQBQ.* 2017; 17 (4) :17-27. <http://mcej.modares.ac.ir/article-16-7139-en.html>
- Taghipour, S., & Ayati, B. (2017). Cultivation of aerobic granules through synthetic petroleum wastewater treatment in a cyclic aerobic granular reactor. *DESALINATION AND WATER TREATMENT*, 76, 134-142. <https://doi:10.5004/dwt.2017.20779>
- Tang M.K.Y., Ng H.Y., 2014. Impacts of different draw solutions on a novel anaerobic forward osmosis membrane bioreactor (AnFOMBR). *Water Sci. Technol.* 69, 2036–2042. <https://doi.org/10.2166/wst.2014.116>
- UN, 2019. United Nations Sustainable Development Goals [WWW Document]. URL <https://www.un.org/sustainabledevelopment/sustainable-development-goals/> (accessed 9.14.19).
- Verrecht B., Judd S., Guglielmi G., Brepols C., Mulder J.W., 2008. An aeration energy model for an immersed membrane bioreactor. *Water Res.* 42, 4761–4770. <https://doi.org/10.1016/j.watres.2008.09.013>
- Wang H., Wang X., Meng F., Li X., Ren Y., She Q., 2019. Effect of driving force on the performance of anaerobic osmotic membrane bioreactors: New insight into enhancing water flux of FO membrane via controlling driving force in a two-stage pattern. *J. Membr. Sci.* 569, 41–47. <https://doi.org/10.1016/j.memsci.2018.10.010>
- Wang K.M., Cingolani D., Eusebi A.L., Soares A., Jefferson B., McAdam E.J., 2018a. Identification of gas sparging regimes for granular anaerobic membrane bioreactor to enable energy neutral municipal wastewater treatment. *J. Membr. Sci.* 555, 125–133. <https://doi.org/10.1016/j.memsci.2018.03.032>
- Wang L., Liu Hongbo, Zhang W., Yu T., Jin Q., Fu B., Liu He, 2018. Recovery of organic matters in wastewater by self-forming dynamic membrane bioreactor: Performance and membrane fouling. *Chemosphere* 203, 123–131. <https://doi.org/10.1016/j.chemosphere.2018.03.171>
- Wang X., Chang V.W.C., Tang C.Y., 2016a. Osmotic membrane bioreactor (OMBR) technology for wastewater treatment and reclamation: Advances, challenges and prospects for the future. *J. Membr. Sci.* 504, 113–132. <https://doi.org/10.1016/j.memsci.2016.01.010>
- Wang X., Wang C., Tang C.Y., Hu T., Li X., Ren Y., 2017. Development of a novel anaerobic membrane bioreactor simultaneously integrating microfiltration and forward osmosis membranes for low-strength wastewater treatment. *J. Membr. Sci.* 527, 1–7. <https://doi.org/10.1016/j.memsci.2016.12.062>
- Wang Z., Zheng J., Tang J., Wang X., Wu Z., 2016. A pilot-scale forward osmosis membrane

- system for concentrating low-strength municipal wastewater: Performance and implications. *Sci. Rep.* 6, 1–11. <https://doi.org/10.1038/srep21653>
- Weerasekara N.A., Choo K.H., Lee C.H., 2014. Hybridization of physical cleaning and quorum quenching to minimize membrane biofouling and energy consumption in a membrane bioreactor. *Water Res.* 67, 1–10. <https://doi.org/10.1016/j.watres.2014.08.049>
- Werner C.M., Katuri K.P., Hari A.R., Chen W., Lai Z., Logan B.E., Amy G.L., Saikaly P.E., 2016. Graphene-coated hollow fiber membrane as the cathode in anaerobic electrochemical membrane bioreactors – Effect of configuration and applied voltage on performance and membrane fouling. *Environ. Sci. Technol.* 50, 4439–4447. <https://doi.org/10.1021/acs.est.5b02833>
- Won Y., Choo K., Lee C., Park P., 2016. More efficient media design for enhanced biofouling control in a membrane bioreactor: Quorum quenching bacteria entrapping hollow cylinder. *Environ. Sci. Technol.* 50, 8596–8604. <https://doi.org/10.1021/acs.est.6b01221>
- Xiong Y., Harb M., Hong P., 2016. Characterization of biofoulants illustrates different membrane fouling mechanisms for aerobic and anaerobic membrane bioreactors. *Sep. Purif. Technol.* 157, 192–202. <https://doi.org/10.1016/j.seppur.2015.11.024>
- Xu, B., Albert Ng, T.C., Huang, S., Shi, X., Ng, H.Y., 2020a. Feasibility of isolated novel facultative quorum quenching consortia for fouling control in an AnMBR. *Water Res.* 169, 115251. <https://doi.org/10.1016/j.watres.2019.115251>
- Xu, B., Ng, T.C.A., Huang, S., Ng, H.Y., 2020b. Effect of quorum quenching on EPS and size-fractionated particles and organics in anaerobic membrane bioreactor for domestic wastewater treatment. *Water Res.* 179, 115850. <https://doi.org/10.1016/j.watres.2020.115850>
- Xue W., Yamamoto K., Tobino T., 2016. Membrane fouling and long-term performance of seawater-driven forward osmosis for enrichment of nutrients in treated municipal wastewater. *J. Membr. Sci.* 499, 555–562. <https://doi.org/10.1016/j.memsci.2015.11.009>
- Yang J., Ji X., Lu L., Ma H., Chen Y., Guo J., Fang F., 2017. Performance of an anaerobic membrane bioreactor in which granular sludge and dynamic filtration are integrated. *Biofouling* 33, 36–44. <https://doi.org/10.1080/08927014.2016.1262845>
- Yang Y., Qiao S., Jin R., Zhou J., Quan X., 2019. Novel anaerobic electrochemical membrane bioreactor with a CNTs hollow fiber membrane cathode to mitigate membrane fouling and enhance energy recovery. *Environ. Sci. Technol.* 53, 1014–1021. <https://doi.org/10.1021/acs.est.8b05186>
- Yang Y., Qiao S., Jin R., Zhou J., Quan X., 2018. Fouling control mechanisms in filtrating natural organic matters by electro-enhanced carbon nanotubes hollow fiber membranes. *J. of Membr. Sci.* 553, 54–62. <https://doi.org/10.1016/j.memsci.2018.02.012>
- Zhang J., Chua H.C., Zhou J., Fane A.G., 2006. Factors affecting the membrane performance in submerged membrane bioreactors. *J. of Membr. Sci.* 284, 54–66. <https://doi.org/10.1016/j.memsci.2006.06.022>
- Zhang X., Wang Z., Wu Z., Lu F., Tong J., Zang L., 2010. Formation of dynamic membrane in an anaerobic membrane bioreactor for municipal wastewater treatment. *Chem. Eng. J.* 165, 175–183. <https://doi.org/10.1016/j.cej.2010.09.013>

- Zhang X., Wang Z., Wu Z., Wei T., Lu F., Tong J., Mai S., 2011. Membrane fouling in an anaerobic dynamic membrane bioreactor (AnDMBR) for municipal wastewater treatment: Characteristics of membrane foulants and bulk sludge. *Process Biochem.* 46, 1538–1544. <https://doi.org/10.1016/j.procbio.2011.04.002>
- Zhang X., Ning Z., Wang D.K., Diniz da Costa J.C., 2014. Processing municipal wastewaters by forward osmosis using CTA membrane. *J. of Membr. Sci.* 468, 269–275. <https://doi.org/10.1016/j.memsci.2014.06.016>
- Zhang, Q., Hu, J., & Lee, D. J. (2016). Aerobic granular processes: current research trends. *Bioresource Technology*, 210, 74-80. <https://doi.org/10.1016/j.biortech.2016.01.098>.
- Zhang H., Jiang W., Cui H., 2017. Performance of anaerobic forward osmosis membrane bioreactor coupled with microbial electrolysis cell (AnOMEBR) for energy recovery and membrane fouling alleviation. *Chem. Eng. J.* 321, 375–383. <https://doi.org/10.1016/j.cej.2017.03.134>